OH RADICAL MEASUREMENTS: THE IMPACT ON POWER PLANT PLUME CHEMISTRY

Final Report
on RP-676
(Report #EA-465)

Submitted to:

Electric Power Research Institute
3412 Hillview Avenue
P.O. Box 10412
Palo Alto, CA 94303

Prepared by:

Dr. Douglas D. Davis
Atmospheric Chemistry Branch
Applied Sciences Laboratory
Engineering Experiment Station
Georgia Institute of Technology
Atlanta, Georgia 30332

NOTICE

This report was prepared by the Applied Sciences Laboratory at Georgia Institute of Technology as an account of work sponsored by the Electric Power Research Institute, Inc. (EPRI). Neither EPRI, members of EPRI, ASL, nor any person acting on behalf of either: (a) makes any warranty or representation, express or implied, with respect to the accuracy, completeness, or usefulness of the information contained in this report, or that the use of any information, apparatus, method, or process in this report may not infringe privately owned rights; or (b) assumes any liabilities with respect to the use of, or for damages resulting from the use of, any information, apparatus, method, or process disclosed in this report.

TABLE OF CONTENTS

Section		Page
I	SUMMARY	1-1
II	OVERVIEW OF RESEARCH PROBLEM	2-1
III	EXPERIMENTAL	3-1
	Description of Georgia Tech OH Probe	3-1
	Other Experimental Measurements	3-16
IV	RESULTS	4-1
V	DISCUSSION OF RESULTS	5-1
	Comparison of Measurements with Theory	5-1
	Calculation of Conversion Rates for SO_2 and NO_2 via Reaction with OH	5-5
VI	CONCLUSIONS	6-1
VII	RECOMMENDATIONS FOR FUTURE WORK	7-1

LIST OF FIGURES

Figure		Page
1	Five homogeneous daytime chemistry zones in fossil fuel power plant plumes	2-3
2	Schematic diagram of OH laser detection system	3-2
3	Georgia Tech OH laser probe mounted on the NCAR Electra	3-3
4	Georgia Tech OH laser probe mounted on the NCAR Electra	3-4
5	OH collection optics	3-6
6	Aircraft OH calibration system	3-8
7	Region of Study	4-2
8	National Center for Atmospheric Research Electra	4-3
9	Flight profile flown to obtain "near" plume ambient OH concentrations	4-5
10	Flight profile flown to obtain downwind plume concentrations	4-6
11	Diurnal fluctuations in the steady-state concentration of atmospheric OH as a function of latitude and altitude	5-7

LIST OF TABLES

Table		Page
I	Summary of OH and related data recorded on July 16 Electra flight	4-8

ABSTRACT

Reported are the first direct measurements of the OH radical in the vicinity of an isolated power plant plume (Four Corners). Since previous field studies by other investigators have suggested that a major fraction of the conversion of SO_2 to sulfate aerosol occurs under very dilute plume conditions, the reported measurements of OH can be realistically used to estimate the conversion time of SO_2 to H_2SO_4 via the $OH+SO_2+M \rightarrow HSO_3$ reaction scheme. The average concentration of OH measured at an altitude of 2.1 km (above sea level) on July 16, 1976 was found to be $9.5\times10^6/cm^3$. A comparison of this value with that calculated from a simple photochemical model (using observational data for the atmospheric variables CO, H_2O, O_3, CH_4, and the UV flux) indicates good agreement between the two within the uncertainties of the model and the measurements. It should be noted, however, that a lack of information on background levels of NO_2 and reactive hydrocarbons, combined with uncertainties which still exist in the definition of the atmospheric degradation scheme for CH_4, preclude any detailed comparison between measurement and theory. If one uses the near high noon value of OH measured on July 16 to calculate the 1/e conversion lifetime for SO_2, a value of 1.4 days is obtained. The latter lifetime would correspond to an SO_2 conversion rate of $\sim$2%/hour. When the lifetime calculation is modified to take into consideration the diurnal cycle of OH, the 1/e conversion lifetime for SO_2 computes out to 4.4 days, giving an apparent overall rate of conversion of $\sim$.7%/hour. Similar calculations carried out for the conversion of NO_2 to HNO_3 give a 1/e lifetime for NO_2 of 3.6 hours. These calculated conversion lifetimes for NO_2 and SO_2 strongly suggest that under warm weather conditions, atmospheric OH should have a very significant effect on the chemistry of power plant plumes.

Section I

SUMMARY

It is generally accepted that one of the major environmental questions related to power plant emissions is that of how to accurately predict downwind H_2SO_4-sulfate aerosol levels. To this end, the present program was initiated to further investigate the possible role of homogeneous gas phase processes in defining power plant plume chemistry. In particular, this study has had as its focal point the direct measurement of the transient chemical species OH (hydroxyl radical). The objective here was that of determining the possible role of this radical species in the chemical conversion of SO_2 to sulfate aerosol and of NO_2 to nitric acid in power plant plumes. In an effort to optimize conditions for making low altitude OH measurements, the Four Corners power plant near Farmington, New Mexico was selected as the sampling site. The methodology employed in making these measurements was that of "laser induced fluorescence." The sampling platform for the OH laser instrument as well as for several other instruments was an L-188C Electra. (This four engine turbo-prop aircraft is owned and operated by the National Center for Atmospheric Research in Boulder, Colorado.) Working also with the Georgia Tech/University of Maryland OH team was a scientific group from Meteorological Research, Inc. This group provided detailed concentration information on several key plume constituents (i.e., NO, NO_2, O_3, SO_2 and $SO_4^=$) as well as a complete definition of the meteorological conditions under which all sampling operations were carried out.

In all, a total of three flights were flown in an effort to gather low altitude OH data near the Four Corners power plant. Only on the last of these flights was significant OH data collected. The direct measurements that were made of OH represent the first ever at low altitudes from an aircraft platform.

In sampling the Four Corners plume, two different flight configurations were employed. The first of these configurations consisted of three 60-70 mile long flight legs flown in an approximate east-west direction paralleling the power plant plume but 10 to 40 miles displaced to the south. The duration of each of

these legs was approximately 13 minutes, and this resulted in approximately eight minutes of OH data collecting. The second flight configuration flown on July 16 consisted of a large number of short flight legs where the sampling path traced out by the aircraft was perpendicular to the power plant plume and the motion of the aircraft was so directed as to ensure that each sampling leg flown was always upwind from the previous sampling leg. In the latter sampling configuration, the location of the plume, and hence the definition of the OH sampling time for each run, was determined by the response of an on-board condensation nuclei counter. (The general location of the plume was established by the MRI aircraft in advance to the arrival of the Electra from Boulder. On July 16 the Four Corners power plant plume was found to be following the San Juan river valley.) Of the two sampling configurations which were tried, only the non-plume profiles resulted in usable OH data. In those sampling runs which involved direct penetration of the plume, we encountered rapidly changing aerosol levels which resulted in rapidly changing scattered light (noise) levels. Since these variations in the noise level occurred at a rate equal to or greater than the OH on-off cycling rate, it was found impossible to retrieve useful OH signal from the system without outrageously long integration times. On the three sampling legs in which OH data were collected, concentration values (for eight-minute integrations) of 9.2, 8.1, and $11.0\times10^6/cm^3$ were measured. The authors do not necessarily believe that these observed variations reflect changing atmospheric conditions, and thus at this time are simply assigning an average value of $9.5\times10^6/cm^3$ for the near high noon OH concentration level.

To compare this measured value of OH with that predicted from a simple photochemical model, several other atmospheric parameters must also be known. If, for example, the principal scheme for producing OH is taken to be the photolysis of O_3, i.e.,

$$(1)\quad O_3 + h\nu \xrightarrow{\lambda<3170\text{A}^{\circ}} O(^1D) + O_2$$

$$(2)\quad O(^1D) + N_2 \longrightarrow O(^3P) + N_2^{\ddagger}$$

$$(3)\quad O(^1D) + H_2O \longrightarrow 2\ OH \quad ,$$

and the possible major loss processes are taken to be reactions (4) and (5)

$$(4)\quad OH + CO \longrightarrow CO_2 + H$$

$$(5)\quad OH + CH_4 \longrightarrow CH_3 + H_2O \quad ;$$

then the OH steady state concentration, to a first approximation, can be expressed in the form of equation V

$$[OH] = [O(^1D)] \frac{2\,k_3[H_2O]}{k_5[CO] - (X-1)k_4[CH_4]} \qquad (V)$$

where $$[O(^1D)] = \frac{J_1}{k_2[N_2] + k_3[H_2O]} \qquad (VI)$$

and the term (X-1) before the CH_4 concentration term indicates the net number of OH radicals resulting from the chemical degradation of CH_3. Thus, using our measured values for CO, H_2O, CH_4, O_3, and the ultra-violet flux, we have calculated OH steady state concentrations for X = 0, 1, and 2 of 1.1×10^7, 1.5×10^7, and $2.2\times10^7/cm^3$, respectively. However, if moderate levels of other chemical species such as NO_2 and high molecular hydrocarbons are added into the system (as loss paths), OH concentration levels could be calculated as low as $6\times10^6/cm^3$. At this time, therefore, we can only conclude that within the uncertainties of the modeling calculations (i.e., $[NO_2]$, [RH], and the value of X) and the experimental measurements good agreement exists between simple theory and observations. Obviously, future experiments of this type must involve measurements of both NO_2 and high molecular hydrocarbons at ambient concentration levels.

Using our measured value for OH of $9.5\times10^6/cm^3$ one can then evaluate the 1/e conversion lifetimes for both SO_2 and NO_2. For the NO_2 system, only the elementary process, $NO_2+OH+M \rightarrow HNO_3$, needs to be considered in the generation of the final product, nitric acid. In the case of SO_2, the situation is not so simple. In this system, several reactions must follow the initiating process ($OH+SO_2+M \rightarrow HSO_3$) before the final product H_2SO_4 is formed. In the latter case, however, there are good grounds for making the assumption that the first step involving the reaction with OH is the rate determining step for the overall reaction sequence. For this condition, the 1/e lifetime can be computed in the same way as for NO_2. The respective equations for both NO_2 and SO_2 are as follows:

$$\tau_{NO_2} = \frac{1}{k_6[M][OH]} \qquad M = N_2 \text{ and/or } O_2$$

$$\tau_{SO_2} = \frac{1}{k_7[M][OH]} \qquad M = N_2 \text{ and/or } O_2$$

Using the above equation, together with an effective bimolecular rate constant for $k_6[M]$ of 8×10^{-12} cm^3/molec/s, thus gives a 1/e lifetime (τ) for NO_2 of 3.6 hours. A similar calculation for SO_2, using 9×10^{-13} cm^3/molec/s for the value of $k_7[M]$, gives 1.4 days as the chemical lifetime for SO_2. In the latter case the OH radical would undergo a substantial change in concentration during a 34 hour

period; thus, a more realistic calculation of τ would involve taking a 24 hour averaged value of OH which turns out to be for our case $\sim$ a factor of three less than the high noon value. Using this diurnally averaged value for OH ($2.9\times10^6/cm^3$) then gives a τ value for SO_2 of 4.4 days.

Although at first glance the OH data collected would appear to be unrelated to power plant plume chemistry, in actual fact they are probably more relevant to understanding the $SO_2 \rightarrow$ aerosol conversion process than would be direct in-plume values of OH recorded at short distances downwind from a power plant stack. The above statement is based on the fact that most observational data to date indicate that the 1/e conversion time for SO_2 to sulfate is at least 24 hours. This would suggest then that whatever chemistry does take place involving SO_2 and OH, it occurs predominantly under very dilute plume conditions at long distances where OH levels would be close to those of ambient air. For the above reasons, these investigators believe that the reported OH data should be of major significance in enhancing our understanding of power plant plume chemistry.

Section II

OVERVIEW OF RESEARCH PROBLEM

The mechanism(s) of conversion of SO_2 to H_2SO_4 and/or sulfate aerosol is presently one of the major environmental questions now requiring a definitive answer from the scientific community. Of particular concern here is the fact that anthropogenic emissions of SO_2 are now believed to be about 35% of the total yearly global atmospheric sulfur emitted into the atmosphere. Thus, the anticipated growth expected in the use of high sulfur-containing fossil fuels may lead us to the point where anthropogenic SO_2 will dominate the global cycle of sulfur through the atmosphere. In addition to the local effects of reduced visibility and health risks from sulfate aerosol formation, such increases in the global sulfur budget could influence both global precipitation patterns and the radiative heat balance of the atmosphere and thus impact upon planetary climate.

Power plants as a major source of SO_2 have been under investigation for 10 to 15 years; and yet, no definitive answer is available on the nature of the SO_2 to sulfate conversion process. At the present time, for example, there exists no mathematical relationship which can be used to reliably predict (to within a factor of 5 to 8) the downwind chemical rate of conversion of SO_2 to aerosol. This uncertainty factor, when combined with the smaller but still significant uncertainty in plume dispersion models, leads to very major uncertainties in predictions of downwind aerosol levels from power plant emissions.

Within the last three years, several new power plant field studies have been reported which suggest either the presence of a broad spectrum of chemical behavior in power plant plumes or significant shortcomings in the measurements reported in field studies of these sources or both. As representative of the distribution of observations and thinking on SO_2 plume chemistry, these authors have briefly discussed three different studies in the following text. These studies are: (a) the EPA-sponsored Project MISTT under the direction of Dr. Rudolph Husar (1977); (b) the Brookhaven project, under the direction of Dr. Leonard Newman (1977); and (c) the University of Maryland/Georgia Tech power plant program, under the direction of Dr. D. D. Davis (1974, 1975, and 1977).

The MISTT program since 1974 has undertaken two detailed field experiments in which the plume from the Labadie Power Plant in St. Louis could be independently tracked from the St. Louis urban plume. On August 14, 1974, the SO_2 to sulfate conversion rate was examined out to a distance of 50 km. In the range of 10-30 km, the conversion rate was found to be between one and two percent; however, this rate jumped to as high as four to five percent at distances between 30 and 50 km. In a second field experiment, in the summer of 1976, the Labadie plume was followed for a distance of 150 km downwind. Preliminary results from this study indicate that between 25 and 100 km, a conversion rate of two percent per hour was observed. Beyond 100 km, the SO_2-to-sulfate conversion rate was found to be significantly reduced.

Newman and associates have extensively examined the behavior of SO_2 in power plant plumes in several states (some 25 to 30 independent field experiments) and have come to the conclusion that, within the precision of their experiments (a factor of two), no conversion of SO_2 to aerosol (beyond that observed at one or two miles) occurs as a function of distance up to drift times of about two hours. The observations by Newman and co-workers were made during both winter and summer months.

Davis and co-workers, as a result of extensive laboratory kinetic studies (Davis and Klauber, 1975), were able to obtain good evidence that for an isolated power plant plume, under daylight summertime conditions, one of the most important homogeneous gas phase reactions responsible for converting SO_2 to H_2SO_4 should be that involving the OH radical, i.e.,

$$OH + SO_2 + M \longrightarrow HSO_3 \qquad (1)$$

$$HSO_3 \xrightarrow[\text{steps}]{\text{multiple}} H_2SO_4 \text{ (gas)} \qquad (2)$$

$$\text{(Kiang, 1973,1977) } H_2SO_4 + H_2O \xrightarrow[\text{nucleation}]{\text{heteromolecular}} H_2SO_4 \text{ (aerosol)} \qquad (3)$$

On the basis of laboratory kinetic studies as well as extensive power plant field investigations (1974, 1975), Davis has suggested an empirical plume model to describe daytime homogeneous chemistry (see Figure 1). For this simple model, it is apparent that the OH free radical is depicted as a critical reaction species which has a major influence on both sulfur as well as nitrogen chemistry. However, it should be noted that the chemistry promoted by the OH radical does not take place until the plume has undergone extensive dilution and plume ozone levels have reached near ambient levels. Depending on the size of a given power plant (especially the level of NO emission) and the stability of the atmosphere, the plume drift time required could be one to five hours.

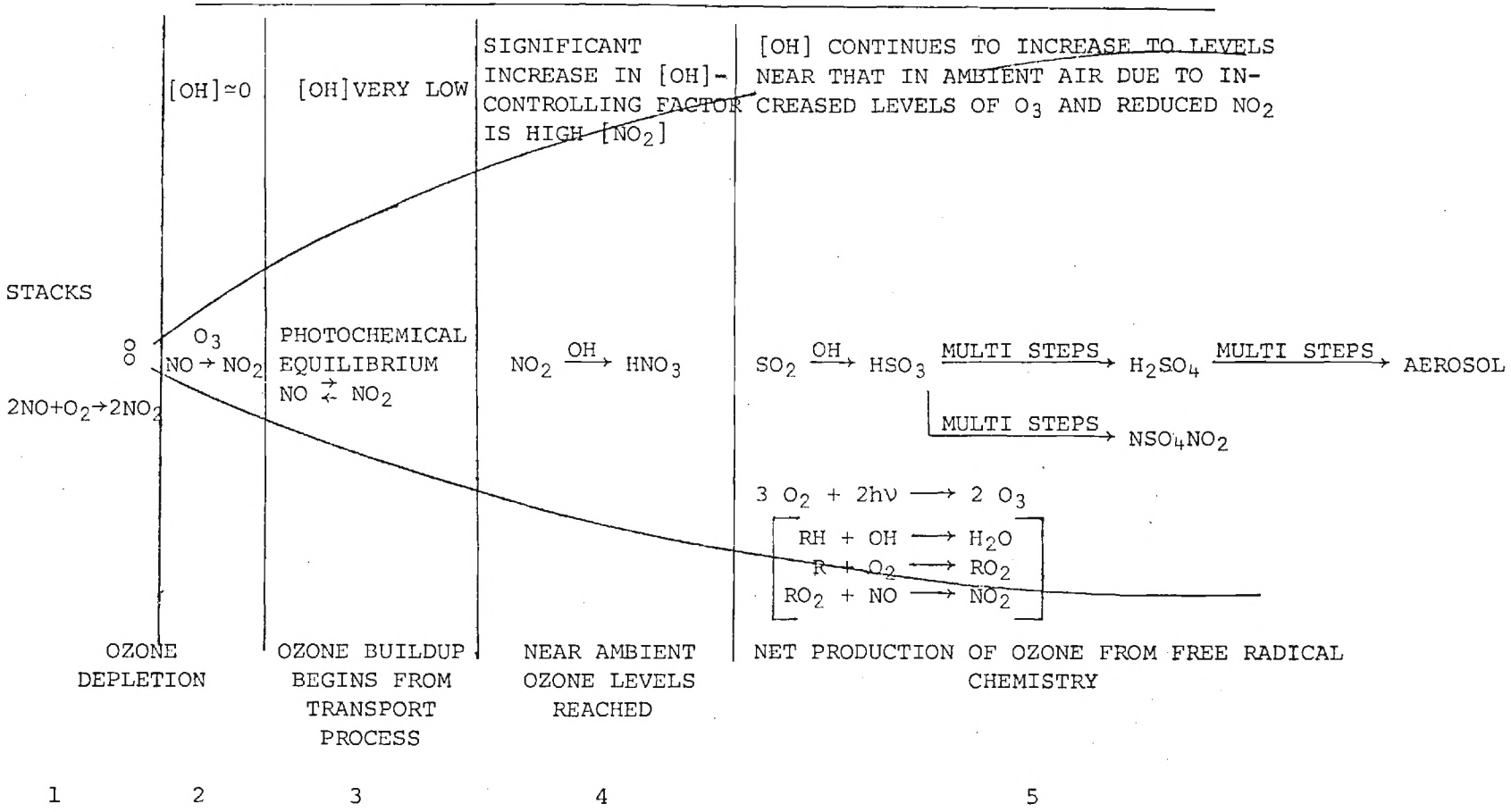

Figure 1. Five homogeneous daytime (Summer) chemistry zones in fossil fuel power plant plumes. All concentration information is referenced to the plume itself.

In the report that follows, the first direct measurements of the OH radical concentration in the immediate vicinity of an isolated power plant plume are reported. These measurements have thus permitted for the first time a realistic calculation of the conversion time of NO_x to nitric acid and most importantly the conversion of SO_2 to H_2SO_4 via the postulated OH mechanism.

Section III

EXPERIMENTAL

DESCRIPTION OF GEORGIA TECH OH PROBE

Introduction

The methodology employed in making the reported direct atmospheric measurements of OH is that of "laser induced fluorescence." The sensitivity of this method is now well documented for OH (Davis et al, 1976 and Davis et al, 1977) as well as several other molecules. In general terms, this technique involves the tuning of a narrow band UV laser to one or more of the electronic absorption bands of a specified molecule so as to cause fluorescence from a bonding excited electronic state. To maximize the signal-to-noise ratio, the fluorescence from this excited state is then monitored at a wavelength somewhat longer than that used to pump the molecule into the excited state.

In the power plant study, where the molecule of interest was OH, the pumping wavelength correlated with the $(^2\Sigma\text{-}^2\Pi)$ 1,0 electronic band. Sampling of the resulting fluorescence was carried out at $\sim$3095Å, using a bandpass filter having a 50Å half-bandwidth. The fluorescence signal sampled consisted of several transitions involving both low K levels of v'=1 and high K levels of v'=0, the latter vibration state being occupied due to collisionally induced vibrational relaxation of the v'=1 state via N_2 and O_2 molecules. In the case of the OH molecule, as well as other molecules that might be detected with the laser induced fluorescence technique, the efficiency with which the excited state fluorescence can be sampled is dependent on both the quenching efficiency of the excited state via N_2 and O_2 and on the wavelength distribution of the fluorescence relative to the sampling width of the bandpass filter. For some molecules (not OH) an additional loss factor can result from a quantum efficiency of less than unity for fluorescence due to predissociation or direct dissociation.

Instrumentation

A schematic diagram showing several of the major components of the Georgia Tech aircraft laser system is shown in Figure 2. In addition, Figures 3 and 4 have

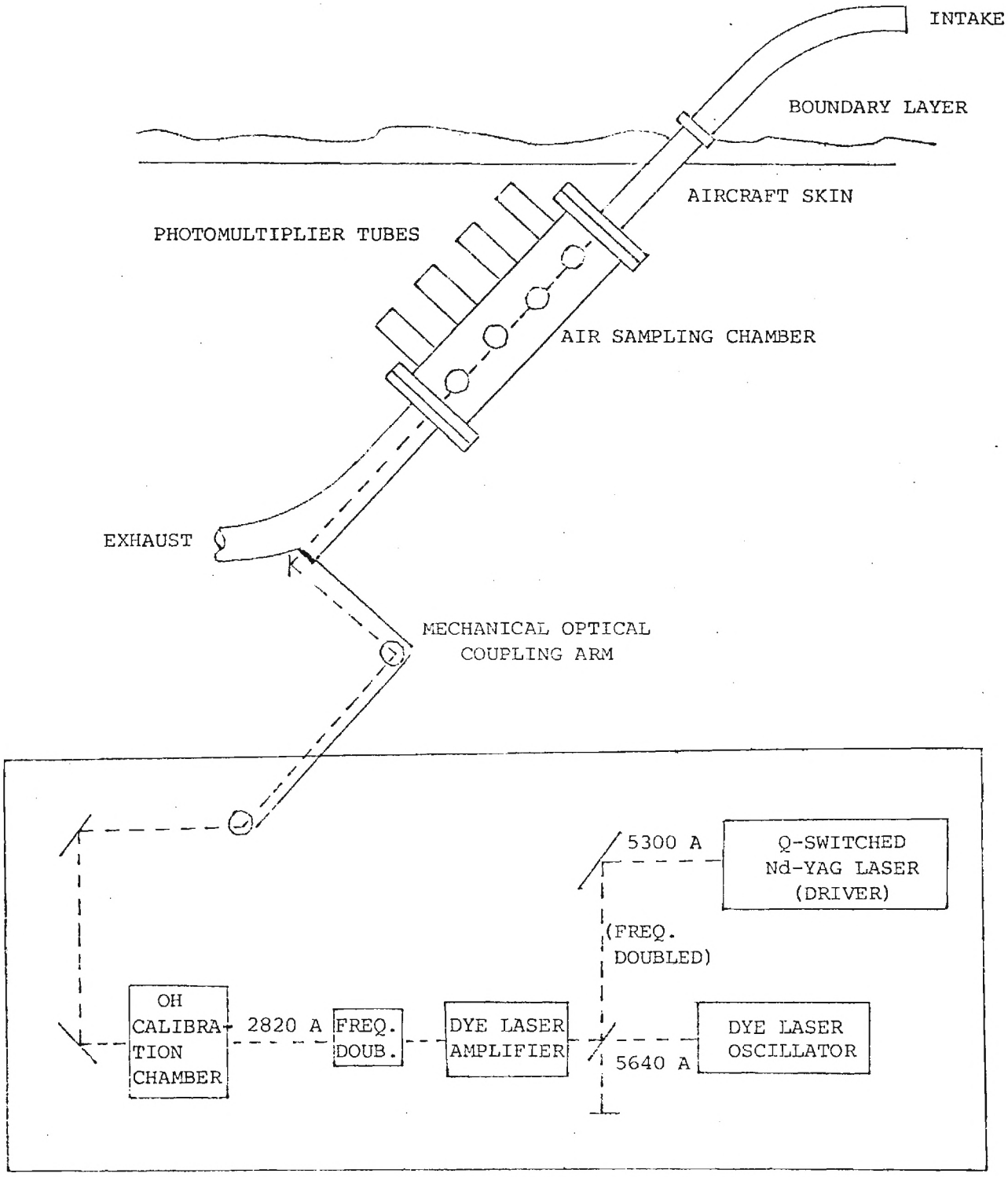

Figure 2. Schematic Diagram of OH Laser Detection System

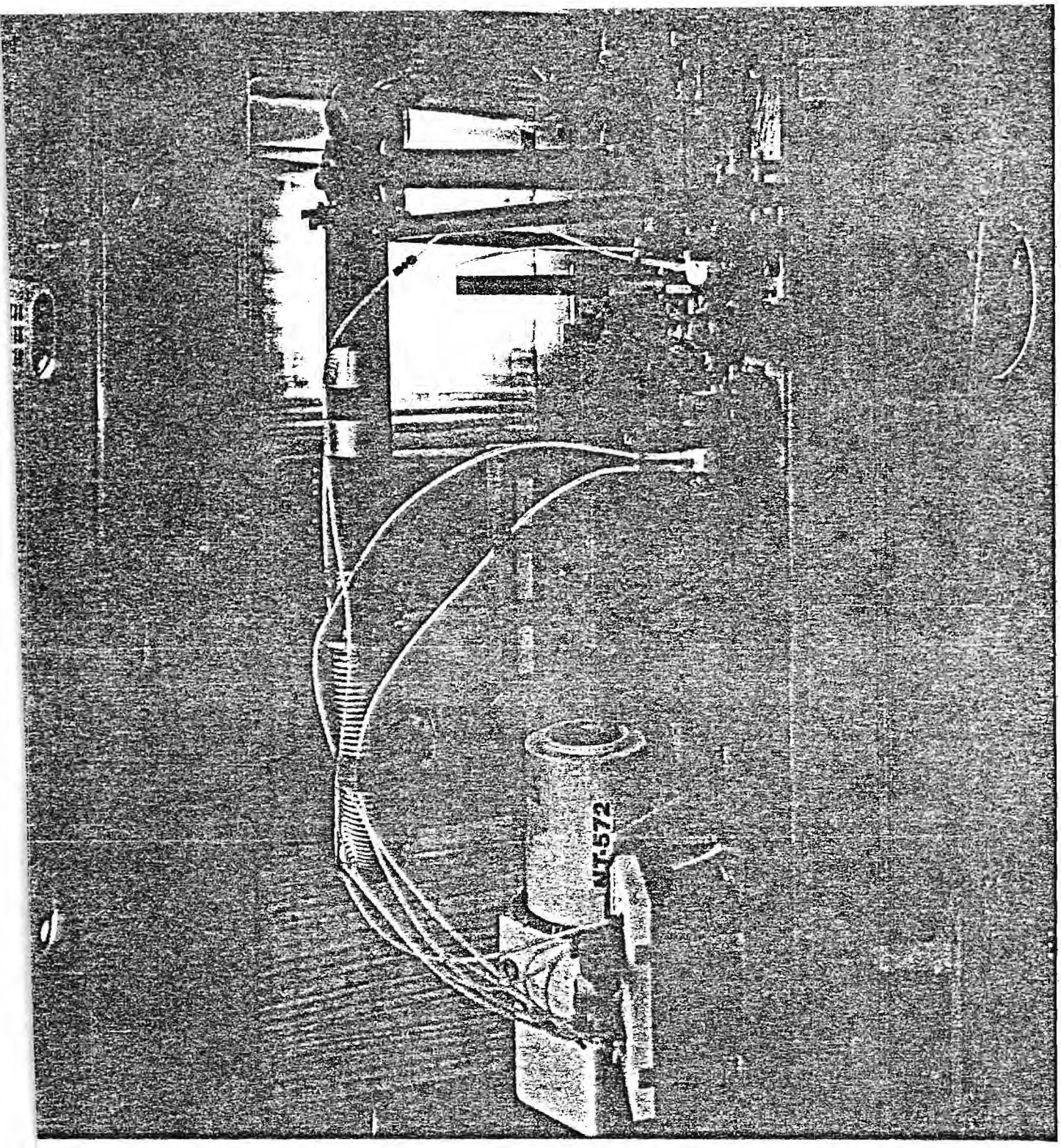

Figure 3. Georgia Tech OH Laser Probe mounted on the NCAR Electra

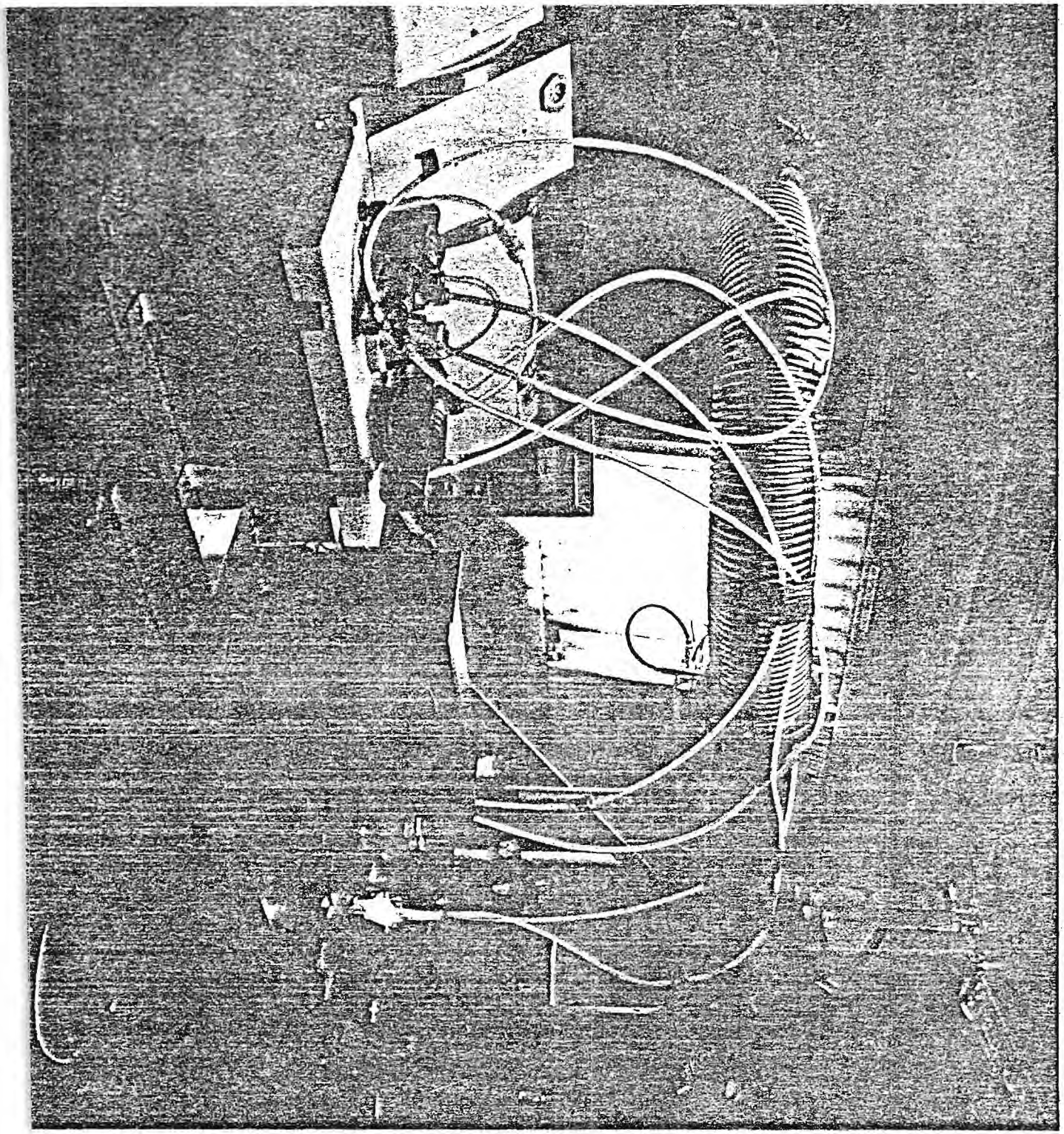

Figure 4. Georgia Tech OH Laser Probe Mounted on the NCAR Electra

been provided to give the reader a more realistic perspective of the OH laser detection system. The photographs shown in these figures were taken while the probe was aboard the NCAR Electra aircraft.

The major components of the OH probe are: (1) an oscillator-amplifier UV tunable dye laser; (2) an air intake-scatter chamber-exhaust system; (3) a mechanical-optical aircraft-to-laser coupling arm; (4) an OH calibration chamber; and (5) signal processing electronics. The first of these major components, the oscillator-amplifier UV tunable dye laser, has been previously described in detail (Moriarty, Heaps, and Davis, 1976, and Davis et al, 1977) and therefore only a brief description will be given here. The Georgia Tech dye laser is an oscillator-amplifier design and utilizes three air gap Fabry Perots for tuning. The dye laser is driven by either a 10 or 20 pulse per second Nd-YAG laser (NT-672 or NT-674) and typically generates UV energy pulses in the .3 to .6 mJ range with a band width of $\sim$.015Å.

The air intake-scatter chamber-exhaust assembly is a completely sealed system which permits high altitude aircraft sampling with a pressurized cabin. The final design of the intake manifold was based on the results from wind tunnel tests on six different designs. The system shown in schematic form in Figure 2 consists of a 3-inch I.D. black anodized aluminum pipe which at speeds in excess of 80.0 m/s displayed a thin turbulent boundary layer along the inner walls but had a non-rotational core flow in a cross sectional region approximately 1-3/4" in diameter but somewhat asymetrically located in the pipe. Since the time of transit to the point of sampling is approximately 12 milliseconds (ms) (the Electra sampling speed being typically 120 m/s), the OH loss due to homogeneous chemistry and/or wall reactions with the intake manifold is negligible. The lifetime of atmospheric OH, for example, is primarily controlled by its reaction with atmospheric CO and CH_4. Thus, taking Northern Hemispheric values of 100 ppbv for CO and 1.5 ppmv for CH_4, results in a lifetime of 1-2s for OH. The radial diffusion time of OH to the walls of the intake manifold, from a centrally located 8 mm diameter beam, varies depending on the atmospheric pressure but would fall generally into the range of 40 to 200 ms over the altitude range of 12 to 2 km. From the above set of numbers, it can be concluded that at the altitude at which all measurements were conducted in the power plant study there should have been no measurable loss of OH in the intake manifold.* All OH measurements completed to date would suggest that the above conclusion is correct.

*To perform this experiment rigorously, OH would have to be carefully measured at two different points in the scatter chamber. A test of this type will be attempted early in 1978.

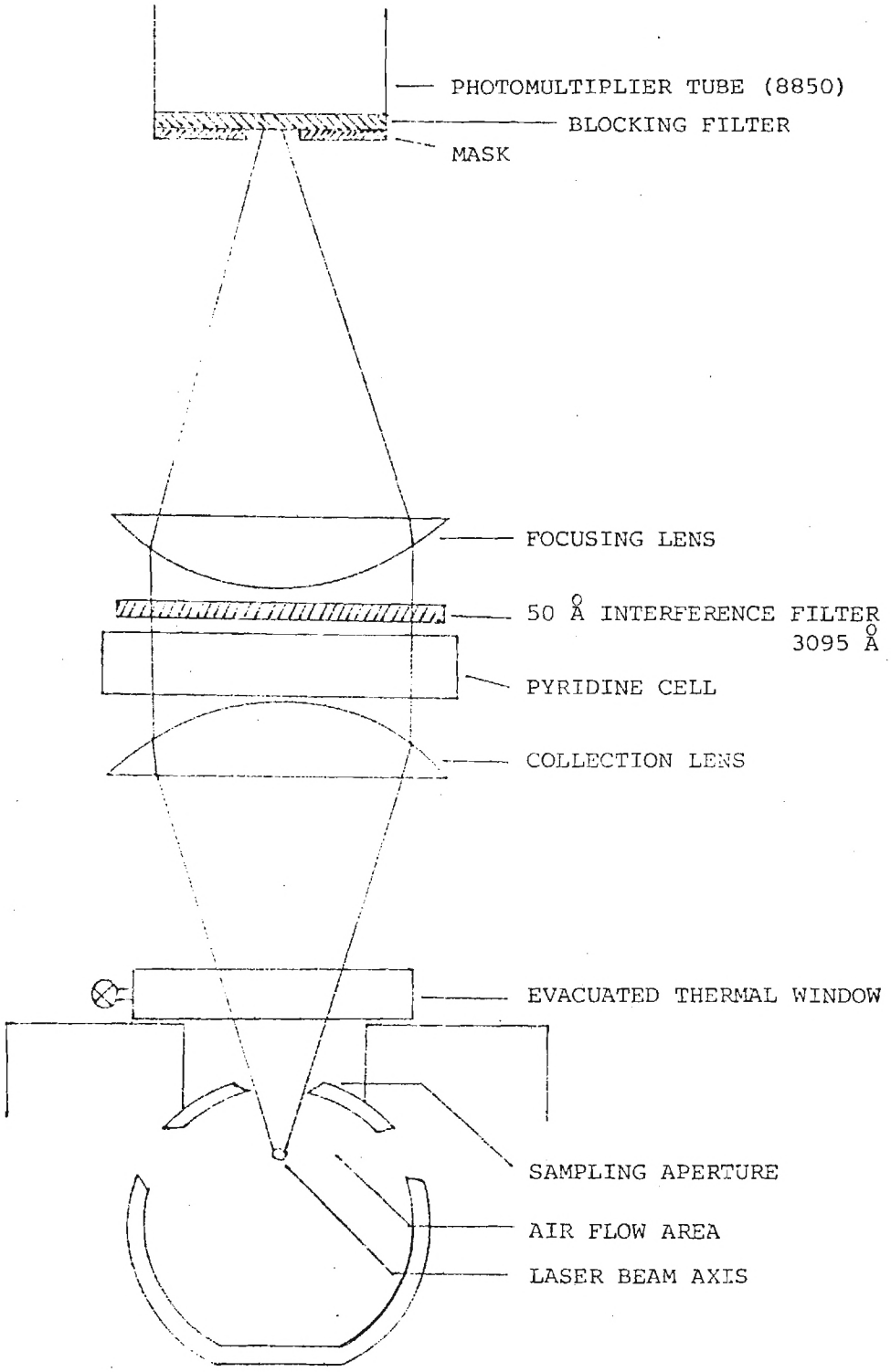

Figure 5. OH Collection Optics: Note, three ports are available for sampling OH fluorescence. Not shown for two of these ports are the thermal windows, collection optics, and PM tubes.

In the aircraft sampling chamber employed during the 1976 experiments, the laser beam was sent through the scatter chamber parallel to the air flow. A total of twelve sampling ports were located on three sides of the .75 meter long chamber. The option existed therefore to run either 12 identical photo tubes (measuring only one species) or several different photo tubes with different filters to monitor multiple species. Because of limited resources, the configuration used in the July-August 1976 flights involved six 8850 photomultiplier tubes dedicated to measuring OH. Details on the collection optics used in front of each tube can be seen in Figure 5. All lenses in this system were made of high quality suprasil quartz. The pyridine cell located between the two lenses served as a low wavelength cut-off filter.

Component (3), "the mechanical-optical coupling assembly" was made necessary due to the fact that the scatter chamber assembly was rigidly attached to the aircraft air frame; whereas, the tunable UV laser was mounted on an optical table which floated on an aircraft vibration isolation system. Thus, to correct for the relative motion between these two elements, a two mirror mechanical linkage system was designed which caused the laser beam to remain stationary despite there occurring translations and rotations about three mutually orthogonal axes. The principal of operation of this steering system is based on the fact that if the angular position of a source and target with respect to a mirror is changed by an angle Θ, the mirror must be rotated by an angle of $\frac{1}{2}\Theta$ in order to redirect the source onto the target. The steering system in this case consisted of two angle bisecting modules coupled together by a rotatable sliding fixture. One of these modules was fixed to the optical table and the other to the sampling manifold. Using precision ball bearings at all pivotal points, the existing beam steering system was capable of holding a given position 2.5 meters away from the source to within 1 to 2 mm under moderate turbulent flying conditions. Tests completed to date show that 3 to 4 mm of displacement could be tolerated without having a significant effect on the signal-to-noise ratio of the OH probe at concentrations of OH of $10^6/cm^3$.

The OH calibration chamber (see Figure 6) served a dual role in the Georgia Tech aircraft system. Firstly, it was used as a frequency locater to establish that the UV laser was either on or off an OH absorption line; and secondly, the calibration chamber was used as an absolute OH standard reference source. Since the first function is satisfied best when the OH signal is strong (i.e., high concentrations of OH and a weak fluorescence quenching environment); whereas, the second function is satisfied with low OH concentrations (approaching those to be measured

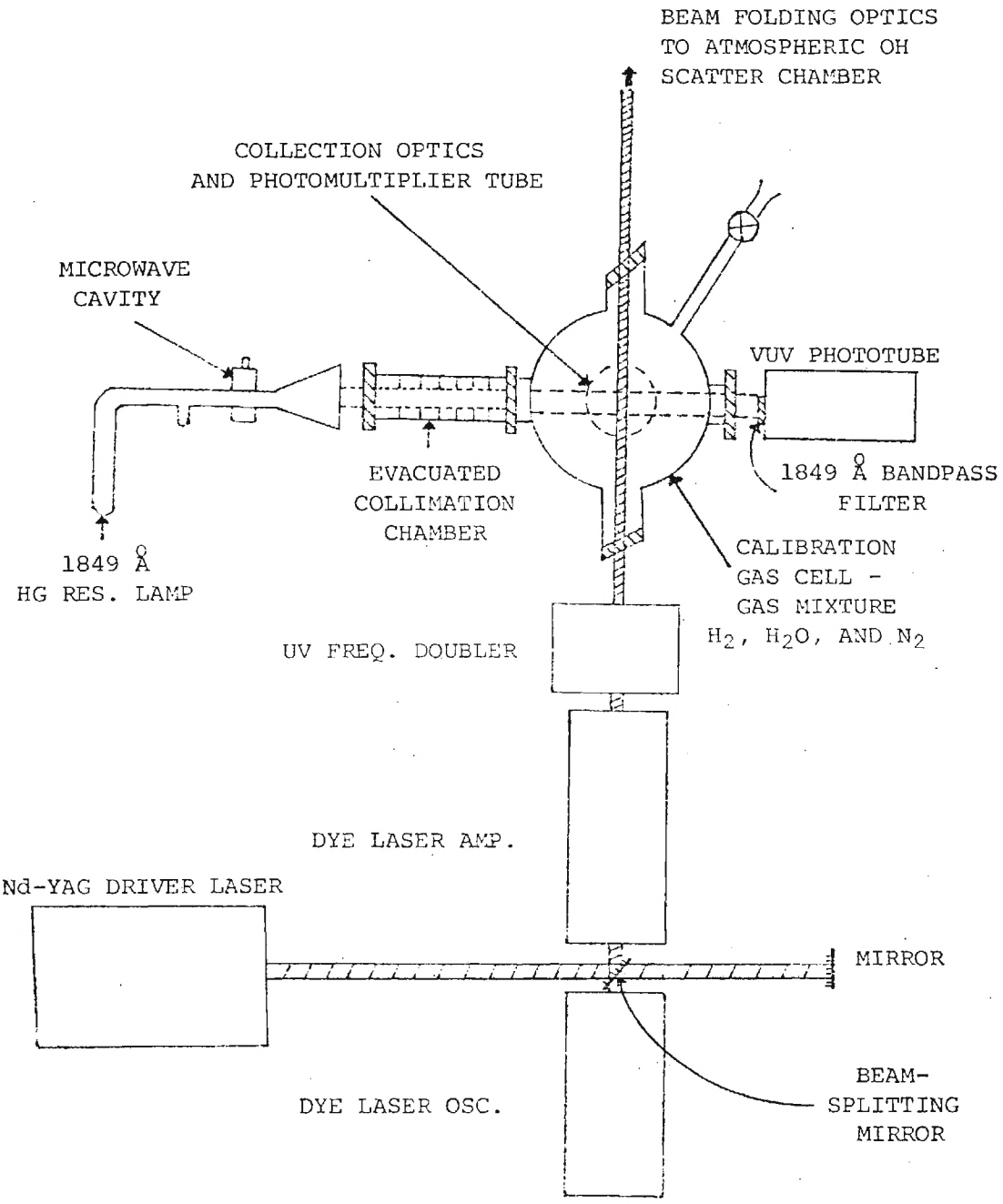

Figure 6. Aircraft OH Calibration System

directly in atmospheric air samples), two different types of calibration chambers were employed. Both chamber types were identical in design (cylindrical quartz cells ~800 cc in volume) and differed only in the composition of the gas mixtures contained within each. The frequency calibration source was filled with H_2O and He (150 mTorr H_2O in 500 Torr of He); whereas, the OH reference source contained an H_2O-N_2-H_2 gas mixture. In both cases, the 1849Å photolysis of water was used to generate a steady concentration of OH. In the frequency source, the OH steady state concentration was controlled by diffusion of OH to the walls and by the incident photon flux from the 1849Å resonance lamp. Typical signal-to-noise ratios for this system were 10:1 for a single laser pulse when using an incident 1849Å photon flux of 3×10^{13} photons/s cm^2. In the case of the OH standard reference source, the relevant reactions which control the steady state OH concentration are:

$$\text{(a)}\quad H_2O + h\nu \xrightarrow{\lambda=1849\text{Å}} OH + H$$

$$\text{(b)}\quad OH + H_2 \longrightarrow H_2O + H$$

$$\text{(c)}\quad H + H + \text{Wall} \longrightarrow H_2$$

Thus, the system has excellent long-term stability since both of the initial reactants H_2O and H_2 are, to a first approximation, continually regenerated. Under photochemical steady conditions, the OH concentration is given by,

$$[OH]_{Cal.} = \frac{I_{abs.}\,\Phi}{k_{H_2}[H_2]} \qquad \text{(I)}$$

where $I_{abs.}$ is the absorbed light intensity by H_2O at 1849Å; Φ is the quantum yield for production of OH from the photolysis of H_2O at 1849Å; and K_{H_2} is the bimolecular rate constant for reaction of OH with H_2. Of considerable importance here is the fact that with four reference cells spanning the N_2 pressure range of 700, 400, 300, and 150 Torr, the atmospheric OH quenching factor is an integral part of the calibration system. (An O_2 quenching factor is also applied.)

The single largest uncertainty in the evaluation of the OH steady state concentration in the calibration cell (see equation I) is that of reliably measuring the 1849Å photon flux. As seen in Figure 6, lamp drift (typically not more than 20-30%) has been resolved by placing a VUV photo tube equipped with an 1849Å bandpass filter directly behind the calibration cell. Thus, the 1849Å photolysis radiation can be continuously monitored, permitting fine adjustments in the value of the photon flux during a given calibration run. This procedure is followed in both the laboratory and on the aircraft. Concerning the absolute measurement of the

1849Å photon flux, N_2O and O_2 chemical actionmetry* have been used. In the N_2O system, the formation of N_2 is used as a measure of the absorbed light intensity. Other experiments using O_2 as the actinic gas, where O_3 production is the product measured, have resulted in photon flux determinations which agree with the N_2O experiments to within 10%. We presently believe that our measurement of the 1849Å flux is no worse than 20% on an absolute scale, but more than likely it is better than this.

Using a range of H_2 concentrations (i.e., a factor of 50) in the H_2O-H_2-N_2 calibration chamber, a linear calibration curve of fluorescence signal versus OH concentration has been generated over the concentration range of 1×10^7 to 5×10^8 OH's/cm^3. The value of 1×10^7/cm^3 does not represent the lower limit of sensitivity for the OH aircraft probe; rather, it reflects the much more limited sensitivity of the calibration chamber which has nearly a factor of 10 higher noise level than the OH aircraft scatter chamber** and the fact that the calibration source has but one phototube versus six on the aircraft chamber. Based on the above calibration curves, we estimate that at low altitudes the aircraft OH sampling system would have a lower limit of detection of 9×10^5 OH's/cm^3 for a signal to noise of 2:1.+

The signal processing electronics in the Georgia Tech system were specifically designed for the OH aircraft sampling probe. The requirement for special electronics was dictated by several factors. (1) The observed lifetime for OH fluorescence is very short because of the extensive quenching by atmospheric nitrogen (it essentially follows the pulse width of the laser, ~8 nanoseconds). (2) The combined effects of quenching and the extremely low natural concentrations of the OH radical give rise to a signal which is less than one photon per laser shot. And (3), the presence of several noise sources (Raman scattering from N_2, fluorescence from the walls of the chamber, and fluorescence from aerosols and to a lesser extent other

---

*In the N_2O system, the absorption of 1849Å radiation by N_2O produces N_2 gas with a quantum efficiency of ~1.4. Thus, by carefully defining the aperature of the photolysis beam and measuring the amount of N_2 produced per unit time of exposure, the photon flux per cm^2 per second can be established. In the case of the O_2 system the photolysis product measured is O_3.

**The reasons for the higher noise level in the calibration chamber versus the aircraft scatter chamber are: (1) higher scattering and fluorescence from quartz versus black anodized aluminum, and (2) the presence of windows close to the sampling aperature in the quartz cell, hence causing higher scatter light.

+ Since the summer flights of 1976, the detection limit of the OH detection system has been further decreased to 3×10^5 OH's/cm^3.

trace constituents)* which collectively generate several photons (2-8 per tube) per laser shot. Under these conditions, photon counting is ruled out because such a system is incapable of counting fast enough to resolve the several background photons plus a possible signal photon which would all appear within ∿8 ns. Thus, in order to generate an output that could be easily interpreted in terms of photons and to take advantage of the extremely short photon emission interval, the following detection technique was implemented.

The output of a photomultiplier tube is allowed to charge a coaxial cable terminated in a resistive load selected to generate a time constant of one microsecond. When the laser fires, a photodiode picks up a trigger signal which, after a suitable delay, causes a fast sample and hold amplifier to sample the voltage on the coaxial cable. (The coax has been chosen for its small capacitance so the charge from the tube can generate a reasonably large voltage on the cable.) The output from the sample and hold amplifier is then converted to a pulse train by a voltage to frequency converter and the pulses are counted for a specified interval by a gated digital counter. This system is calibrated by determining the sampled voltage which generates one count on the gated counter and by establishing the average voltage produced by a single detected photon. The above system has the ability to accept inputs (without switching in voltage divider networks) ranging from a few millivolts to five volts. Since an average single photon is about twenty millivolts, this means that the Georgia Tech system has the ability to count from one to fifty photons per gating interval. Further expansion of the dynamic sampling range and the long term integrating capacity** of this system has been achieved by switching in a divide by 10 analogue voltage divider on the input and by activating a divide by 10 or 100 in the digital counting circuitry.

Of considerable importance here is the short delay time of the coax cable. The one microsecond time constant permits rather selective sampling of the laser induced signal from the photomultiplier tube. For example, any current generated more than two or three microseconds prior to the opening of the sampling gate is effectively lost. By proper adjustment of the trigger to sampling delay, the system can be made to look predominantly at the fluorescence during and immediately following a given laser pulse. Although the RC time constant of the coax could be

---

*The signal generated by scattered solar flux is made much smaller than nearly all other noise sources due to the nature of the gated sampling electronics.

**Integrating capacity in this case means the number of laser shots that can be stored on the digital counters.

made either longer or shorter by selection of the proper resistances, the value of one microsecond has been chosen in the Georgia Tech system as a compromise between minimizing the signal from scattered solar flux and allowing adequate time for the sample and hold to measure the voltage on the coax cable.

The final electronics system which was interfaced with the OH probe consisted of six channels, three of which were used to monitor six RCA 8850 PM tubes and two others to monitor the laser and resonance lamp UV outputs. All major electronic components in this system were spring loaded and mounted in a thermally regulated chassis which provided maximum temperature stability in the event of a changing aircraft cabin temperature.

Data Processing

The working expression which relates the measured aircraft fluorescence signal to the absolute atmospheric OH concentration is given here in the form of equation II.

$$\left(\frac{OH_{Sig}}{[OH] \times UV \times L.S.}\right)_{Cal.C.} = \left(\frac{OH_{Sig}}{[OH] \times UV \times L.S.}\right)_{Prb.} \qquad (II)$$

Upon rearranging equation II, and adding an additional term which takes into account the fact that the efficiency of the collection optics in the calibration chamber and the aircraft probe differ, equation III is generated, i.e.,

$$[OH]_{Prb.} = \frac{(OH_{Sig})_{Prb.} \times [OH]_{Cal.C.} \times (UV)_{Cal.C.} \times (RCE) \times (L.S.)_{Cal.C.}}{(OH_{Sig})_{Cal.C.} \times (UV)_{Prb.} \times (L.S.)_{Prb.}} \qquad (III^*)$$

In equation III,

$(OH_{Sig})_{Prb.}$ = the photon signal generated in the aircraft scatter chamber

$(OH_{Sig})_{Cal.C.}$ = the photon signal generated in the calibration chamber

$[OH]_{Cal.C.}$ = OH concentration in the calibration chamber

$(UV)_{Cal.C.}$ = ultraviolet laser energy incident on the calibration chamber

$(UV)_{Prb.}$ = ultraviolet laser energy incident on the aircraft scatter chamber

*No pressure terms appear in equation II or III since calibration chambers are available which have been filled to gas pressures comparable to that encountered in actual experimental runs.

$(L.S.)_{Cal.C.}$ = the line strength of the OH quantum transition under calibration chamber conditions

$(L.S.)_{Prb.}$ = the line strength of the OH quantum transition under aircraft scatter chamber conditions

(RCE) = the relative collection optics efficiency factor between the calibration chamber and the aircraft probe (e.g., (Coll. optics)Cal.C./(Coll. optics)Prb.)

In equation III, the determination of the number of signal photons derived from an OH source, either the calibration cell or the aircraft probe, requires first a measurement of the OH signal + noise with the laser tuned to the OH absorption line, and then a measurement of the noise only by tuning the laser off the OH frequency. In the Georgia Tech system, the total change in wavelength in the on and off positions is typically only .03 to .04 Å, and this can be achieved in approximately five seconds. To build up a statistically significant number count, integration times of one to ten minutes* have been used (this corresponds to 1200 to 12,000 laser shots at 20 pps). To a first approximation, the probable error in the number of photons detected is then given as the square root of the square of the uncertainty in the signal + noise photons plus the square of the uncertainty in the noise photons,

$$.67\sqrt{\sigma^2_{(\text{signal + noise})} + \sigma^2_{(\text{noise})}}$$

The relative collection optics efficiency factor involving the calibration cell and the aircraft sampling probe has been both calculated and measured experimentally. The experimental measurement is based on the signal observed in each chamber due to Raman scattering from CH_4.** All six PM tubes, together with their respective optics, have been compared with the PM tube and optics in the calibration cell. In these tests, a single tube is also used on each set of collection optics on the aircraft probe to separate collection and transmission effects from varying tube characteristics. In the final analysis, for a given fixed CH_4 pressure, the absolute number of photons measured on the calibration chamber system is compared with the total number of photons measured by the aircraft probe. It is the ratio of these numbers then that defines the quantity RCE.

---

*One to ten minutes is the total time of integration. For ideal averaging, the system is switched on and off frequency every five seconds.

**In these experiments the same bandpass filter is used as in the measurement of OH.

Another term in equation III which has not been previously discussed is the UV laser energy. The absolute UV energy in the Georgia Tech system is measured using a Laser Precision Company UV radiometer which reads the laser energy out directly for each laser pulse. The calibration on this system is directly traceable to NBS, and it is systematically recalibrated every two months. For continuous monitoring of the relative UV energy, a solid state UV photodiode is employed. This system has been exhaustively checked against the absolute UV monitor for both linearity and the absence of any polarization problems. Our best estimate is that the combined systematic error in the quantities (UV) and (RCE) is no worse than 40-50% and more likely is ~15%. A final term in equation III which needs further explanation is (L.S.). This term must be used in the calculation of $[OH]_{Prb.}$ any time the temperature of the air being sampled is significantly different than that of the calibration chamber. The net effect of this temperature difference is that of changing the rotational distribution of the OH ground electronic state, and hence, the number of OH molecules which can be excited to fluorescence for a given UV laser energy. A direct measurement of the temperature (to within $1^{o}C$) permits the calculation of the (L.S.) term to better than 5%.

Interferences

By its basic spectroscopic nature, the laser induced fluorescence method of detecting OH is very highly specific for OH. Although some atmospheric substances may fluoresce upon being excited with 2819Å radiation, in virtually all cases examined this induced fluorescence does not change upon tuning the laser .04Å, as does the OH fluorescence. Thus, such fluorescing substances appear as white noise and therefore can be handled like all other sources of white noise (i.e., Raman scattering from N_2 and chamber wall fluorescence). Species which have been examined for possible interference are SO_2, CH_2O, aromatic hydrocarbons,* and aerosols. A simple mathematical relationship which enables one to evaluate the interference level is given by equation IV.

$$\text{**Interference Factor for Species A} = \frac{\left(\sigma_A\right)\left(\text{Contrast Factor}\right)_A\left(\text{Bandwidth Samp. Eff.}\right)_A\left(\Phi_F\right)_A Q_A}{\left(\sigma_{OH}\right)\left(\text{Contrast Factor}\right)_{OH}\left(\text{Bandwidth Samp. Eff.}\right)_{OH}\left(\Phi_F\right)_{OH} Q_{OH}} \qquad \text{(IV)}$$

*The aromatic species examined were toluene, napthalene, anthracene, and phenanthrene.

**The interference factor times the concentration of species A gives the concentration of OH that species A would appear as in the final integrated signal.

where σ_A and σ_{OH} are the absorption cross sections for species A and OH; the contrast factor for A is given by the ratio

$$\frac{\left(\begin{array}{c}\text{signal from A when}\\ \text{laser is on OH line}\end{array}\right) - \left(\begin{array}{c}\text{signal from A when}\\ \text{laser is off OH}\end{array}\right)}{\left(\begin{array}{c}\text{signal from A when}\\ \text{laser is on OH line}\end{array}\right)}$$

the bandwidth sampling efficiency for A and OH is a measure of what fraction of the total fluorescence for each species passes through the 50Å bandpass at 3095Å; $(\Phi_F)_A$ and $(\Phi_F)_{OH}$ are the fluorescent quantum yields for each species; and finally, Q_A and Q_{OH} are related to the atmospheric quenching factors for species A and OH. Calculations based on 20 ppbv of gaseous species such as SO_2 and CH_2O show that no significant interference with OH measurements would result until OH levels as low as 10^3 to 10^4 were reached.

With regards to aerosols, the information needed to evaluate equation IV is not on hand. The experience of the Georgia Tech group is that aerosols typically result in the generation of white noise source. A special type of interference which developed in this study, however, was that resulting from the variability in the aerosol concentration as observed on board the aircraft as it traversed the power plant plume. Since scattered light from plume aerosol was the principal source of noise in the OH probe, the rapid change in the aerosol level (as compared with the on and off OH frequency cycling time) as the aircraft passed through the plume at 200+ knots/hour produced a rapidly oscillating noise level. The consequences of this phenomenon will be discussed later in the report under the section labelled "Results."

A final interference problem that can not be assessed by equation IV is that involving the artificial generation of OH via laser beam photolysis of O_3 in the presence of H_2O (i.e., $O_3 + h\nu \rightarrow O(^1D) + O_2$ followed by $O^1D + H_2O \rightarrow 2\ OH$). This phenomenon has been extensively researched by our group and on the basis of laboratory test as well as day-night field test (Davis et al, 1976) we have demonstrated that this interference problem is unimportant in our system when the laser energy is <.5 mJ, the pulse width is 8 ns, the beam diameter is ∿5 mm, the humidity is <70% at temperatures of 25°C, and the ozone concentration is less than 100 ppbv. Unimportant, in this case, means that extrapolations of laboratory data would put the artificial generation of detectable OH under the above conditions at $3\text{-}4\times10^5$/ cm^3.

OTHER EXPERIMENTAL MEASUREMENTS

Ozone

Ozone measurements aboard the Electra aircraft were carried out using a Model 1003AAS Dasibi ozone analyzer. The Dasibi instrument monitors ozone on a continuous basis through the use of a long pass UV absorption cell. The light source in this system is a 2537Å Hg lamp. To obtain a constant check on lamp or electronic drift, the Dasibi instrument continuously compares the signal from the sample cell to that of an identical reference chamber. Since the gas stream flowing through the reference cell is first scrubbed of all ozone, the difference in the signal from the reference cell to that in the sample chamber is a true measure of the absolute ozone concentration. Sensitivity: 3 ppbv; precision, ±1 ppb.

H_2O and/or Humidity

Two measuring devices were used on board the Electra during this study. Both systems are standard equipment on the Electra and thus are maintained and operated by NCAR. The first type of instrument, a thermoelectric hygrometer, measures the atmospheric water content by determining the temperature at which a mirror inside the instrument (exposed to outside air) produces a fogged surface. Hence, the quantity measured by this device is the dew point which when combined with the absolute temperature can be converted to atmospheric water content. Sensitivity: 50 to +50°C; precision, ±0.1°C.

The second type of water sensor on the Electra is a Lyman-Alpha Hygrometer. This instrument measures the absolute amount of water in the atmosphere in terms of gH_2O/kg dry air. The method of measurement in this instrument is that of absorption of 1216Å Lyman-Alpha radiation directly by H_2O. This measurement is possible due to the extremely small value of the absorption coefficient (σ) for O_2 at 1216Å and the corresponding large value of σ for H_2O at this same wavelength. Small corrections need to be made for the changing O_2 content with altitude. Sensitivity: 0 to 40 gH_2O/kg dry air; precision, ±.01 g/kg.

CO and CH_4

Both CO and CH_4 were measured via the grab sampling technique. (Leroy Heidt of NCAR carried out the analysis of all grab samples.) The technology involved in grab sampling is now well established as is the gas-liquid chromatographic analysis of CO and CH_4. To maximize the sensitivity for CO, a catalytic cell was added to the end of the GLC elution column. The latter element converts CO to CH_4 which has

a better response to flame ionization detection. Sensitivity CO: 20 ppb; precision, ±7 ppb. Sensitivity CH_4: 30 ppb; precision, ±10 ppb.

Ultraviolet Solar Radiation

The critical region of the UV spectrum which affects the steady state concentration of OH is from 2850 to 3180Å. However, because of the rapidly changing solar flux with wavelength, the rapidly changing absorption cross section for O_3 with wavelength, and the rapidly changing quantum yield for production of $O(^1D)$ atoms as a function of the photolysis wavelength, useful UV measurements can only be obtained if the UV flux is monitored in 20-30Å bandwidths throughout the spectral region of 2850 to 3180Å. Although during the power plant plume study no such instrument was available, an instrument designed and manufactured by Panametrics was flown on the Electra in the same geographical area approximately two weeks later. The measurements made in that case involved a different NCAR program. Since on both occasions the cloud coverage was slight, we believe that the later UV measurements are, in all likelihood, a very good representation of the effective UV flux for that time of year and that geographical location.

Aerosol

Aerosol measurements were made using a Rich 100 Condensation Nuclei Counter (commercial instrument). The reasons for having this instrument on board the Electra during the power plant plume study were twofold: (1) it provided a sensitive method for determining when the aircraft was in the power plant plume, and (2) it enabled us to correlate rapidly changing aerosol levels with apparent OH signal-to-noise ratios. Typically the integration time constant on the CN counter was 5 to 20 times shorter than for the OH instrument.

Pressure

A pressure transducer is part of the permanent equipment aboard the NCAR Electra. Range is 300 to 1035 mb.

Altitude

Altimeters are standard equipment on the Electra. Continuously recorded.

Wind Velocities

U, V, and W wind speeds are continuously measured on the NCAR Electra using a specially designed gust probe mounted on the nose boom of the aircraft.

Section IV

RESULTS

A total of four flights were carried out during this power plant field study. The first of these flights was a short shakedown operation to establish the basic integrity of the OH probe on board the Electra. This flight was, in fact, the maiden flight for the OH laser system aboard the Electra. Several optical, mechanical, and electronic problems were identified during this test flight. Two days were required to modify the OH system to resolve these problems. The first plume flight involving the Four Corners Power Plant (Farmington, New Mexico) was initiated on July 11, 1976 (see Figure 7 for location map). The NCAR Electra aircraft (see Figure 8) on this flight operation was flown at ~6.0 km while traversing the Rocky Mountains and as Farmington, New Mexico was approached, the altitude was reduced to 0.5 to 0.8 km above the surface terrain. The aircraft then proceeded to a quadrant southwest of the Four Corners Power Plant (see Figure 7). On the basis of information given to us by the MRI scientific team, this southwestern quadrant positioned us out of the plume and made it possible to obtain ambient air measurements of OH contiguous to the power plant plume. At the start of this first field experiment, the aircraft experienced moderate turbulence and thus it was essential that the "mechanical-optical coupling assembly" work smoothly. In fact, shortly after the start of our first sampling run, this device locked up and the mission had to be aborted. Upon returning to NCAR, the entire coupling assembly was removed from the aircraft and modifications were made on several critical components of this system. No useful data was obtained on this flight.

On July 14, 1976, the second power plant flight was initiated and on this operation a problem developed with the tunable dye laser. As noted earlier, the Georgia Tech dye laser system is driven by a solid state Nd-YAG laser--frequency doubled to 5300Å. This driver laser (although a state-of-the-art system) is the major weakness in the present dye laser design. During the second flight, a serious failure was experienced with the driver laser. This failure occurred while the aircraft was crossing the Rocky Mountains and all efforts to repair the laser in flight were unsuccessful. Mission number two also had to be aborted, therefore, without the

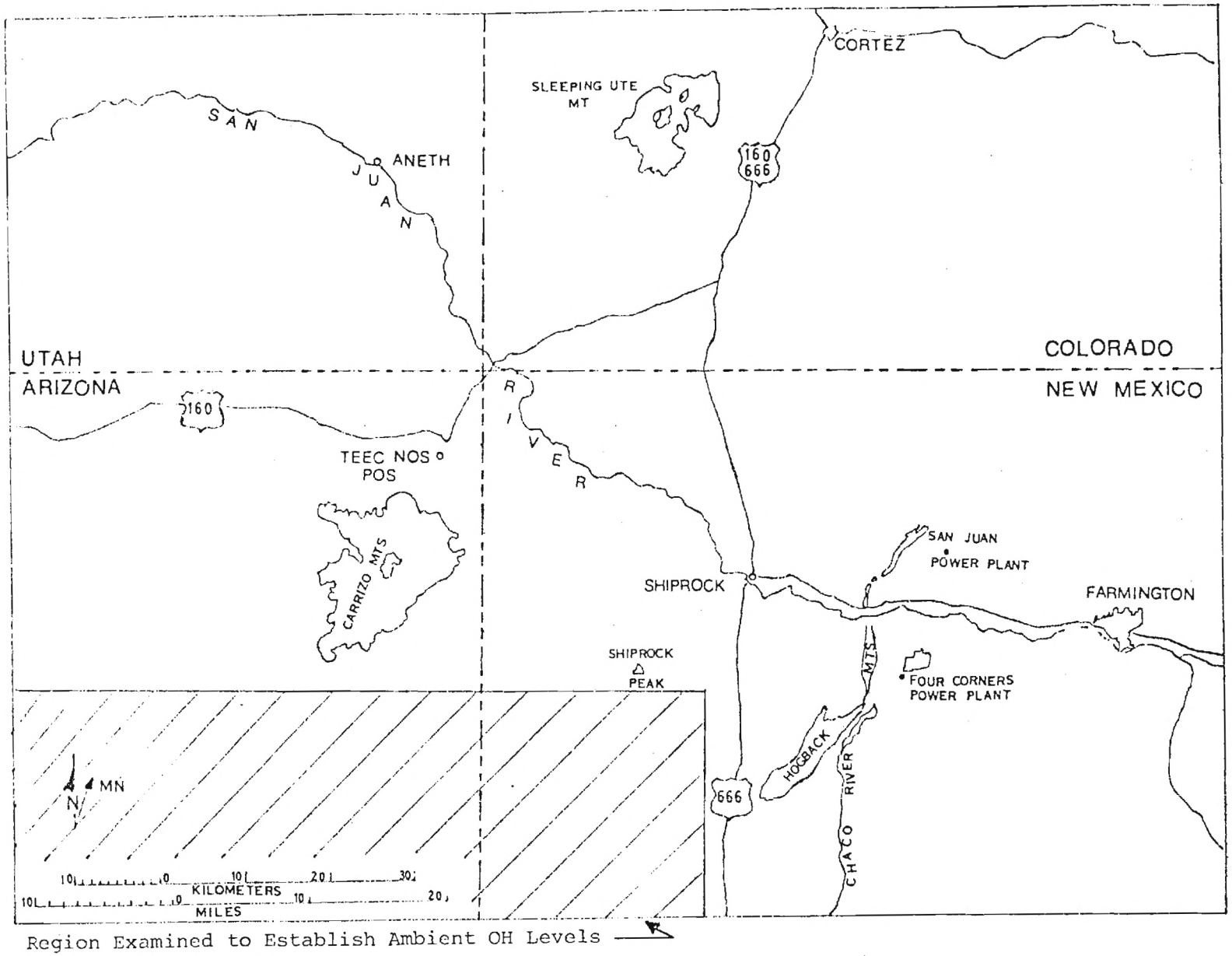

Figure 7. Region of Study

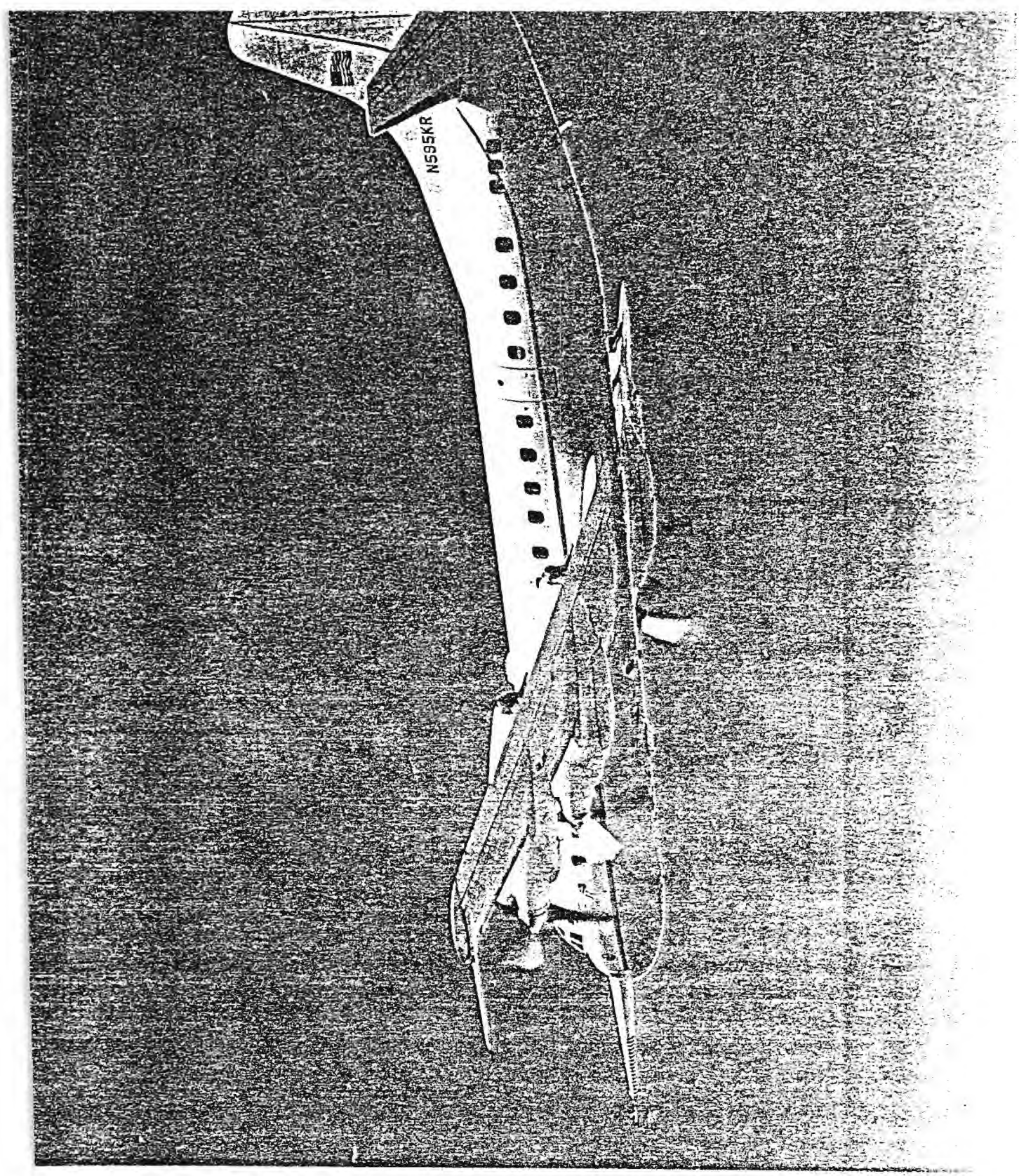

Figure 8. National Center for Atmospheric Research Electra

collection of any OH data. Once the aircraft had returned to NCAR and the driver laser could be inspected more closely, it was soon established that the damage incurred was sufficiently serious as to preclude any immediate repair of the system at NCAR. It was decided, therefore, to remove this system and replace it with a back-up Nd-YAG laser which was borrowed from EPA at Las Vegas.

On July 16, the entire OH laser system functioned without a flaw enabling us to gather OH data both going over the Rocky Mountains at 6.0 km and at low altitudes, 2.1 km (0.7 km above terrain), in the vicinity of the Four Corners Power Plant. While in the Four Corners Power Plant area, two separate types of sampling profiles were flown. The first profile is shown in schematic form in Figure 9 and shows a sequence of three 60-70 mile long flight-legs flown in an approximate east-west direction somewhat paralleling the power plant plume (see Figure 7 for more exact geographical location), but 10 to 40 miles displaced to the south of the plume. The duration of each leg was approximately 13 minutes.

The second flight profile flown on July 16 is shown in schematic form in Figure 10. In this case, the Electra was flown in a pattern consisting of a large number of short flight-legs where the sampling path traced out by the aircraft was perpendicular to the power plant plume and where each subsequent flight-leg flown was always upwind from the previous flight-leg. The location of the plume, and hence the definition of the OH sampling time for each run, was defined by the response of the on-board condensation nuclei counter. The MRI aircraft also informed the Electra pilots of the general location of the plume which was basically the San Juan river valley.

As noted earlier in the text, a major interference encountered in sampling OH directly in the Four Corners Power Plant plume was the rapidly oscillating aerosol level observed when the aircraft crossed the plume perpendicular to its drift vector. These oscillations were in the same frequency time range as the on and off frequency tuning time for the OH probe. Thus, although aerosol scatter is typically a manageable problem as a noise source (white noise), in the case of a power plant plume it behaves like an oscillating noise which in order to signal average out would necessarily require very long integration times. Concerning the flight on July 16, approximately 35 minutes of in-plume data were recorded. With the highly variable noise observed on and off the OH resonance frequency (5 sec sampling times were employed here), we have estimated that at least 900 minutes of data would have been required to extract a believable OH signal for an actual OH

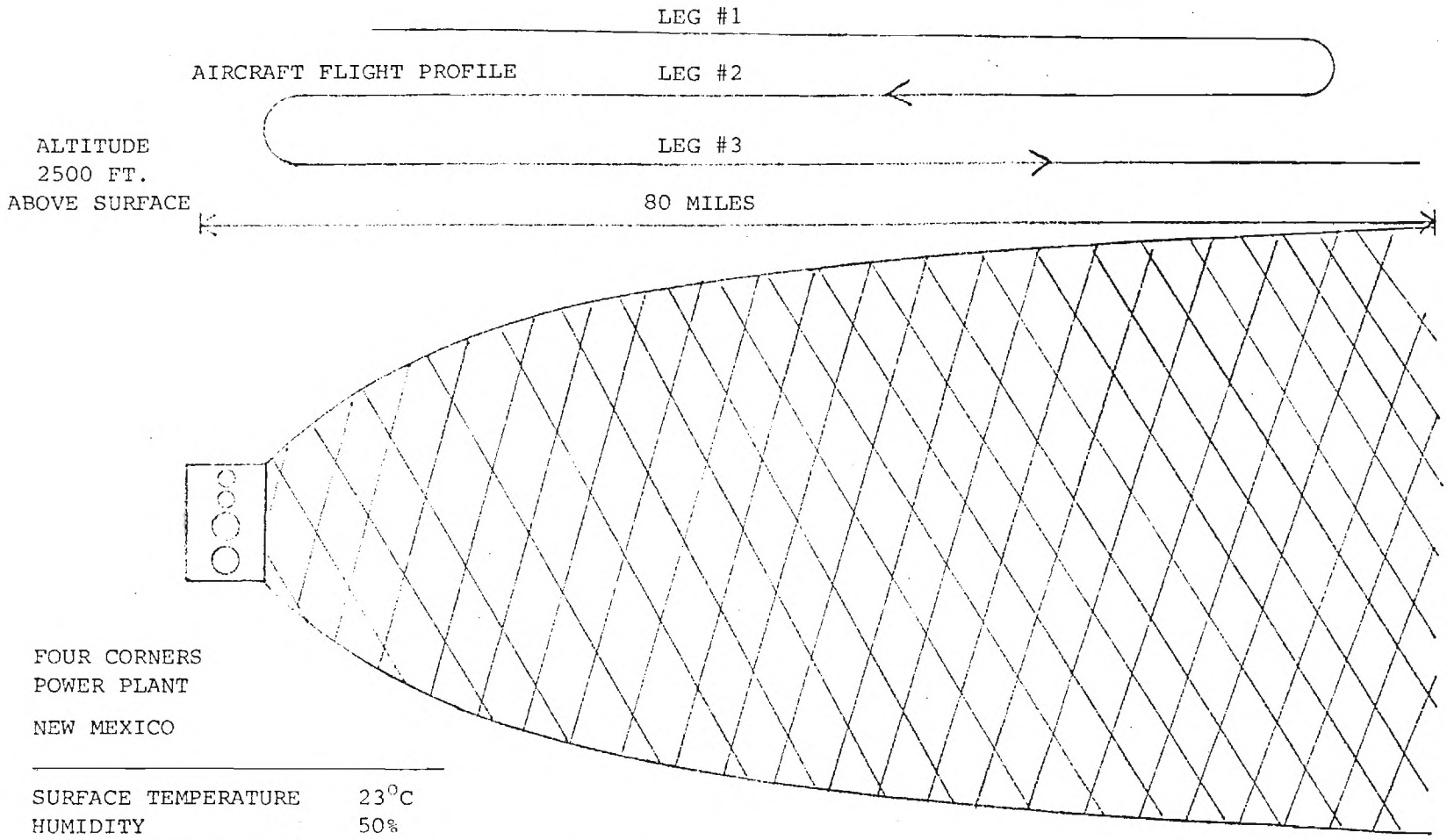

Figure 9. Flight Profile Flown to Obtain "Near" Plume Ambient OH Concentrations

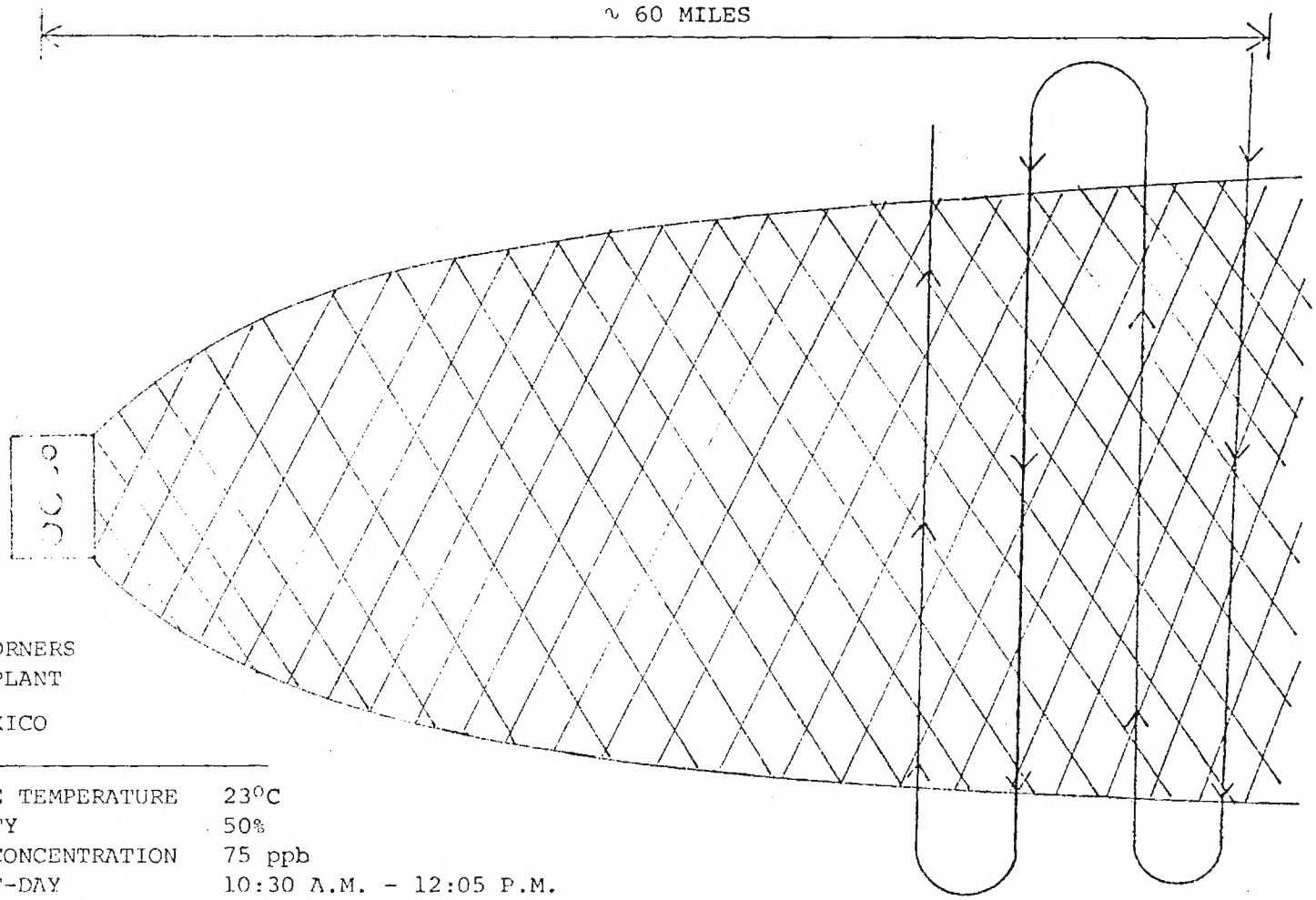

Figure 10. Flight Profile Flown to Obtain Downwind Plume Concentrations

concentration of $9\times10^6/cm^3$. However, as will be discussed in the recommendation section of this report, a modified procedure has now been identified for overcoming the variable in-plume aerosol problem. This alternate approach will not require unrealistic integration time.

With regard to the OH data collected in the "near" plume flight configuration and also at high altitudes over the Rocky Mountains, this information along with related data is summarized here in the form of Table I. It should be noted that the ozone data are those recorded by MRI,* and the UV flux values reported together with the photochemical rate constant, J, are those deduced from the Panametric's measurement two weeks after the power plant plume flight.

From Table I, it can be seen that on three separate runs measured OH values varied from 8.1 to $11.0\times10^6/cm^3$. We do not believe that these variations necessarily reflect changing atmospheric conditions, and at the present time are assigning an average value of $9.5\times10^6/cm^3$. The random error assigned to this average is $\pm2.0\times10^6$ OH/cm^3 and reflects the uncertainty in the calibration procedure and the signal/noise ratio from individual measurements.** It is quite significant, we believe, that the OH value dropped from 9.4 to 3.3×10^6 with a change in altitude. This drop primarily reflects the much lower absolute water content of the atmosphere at the higher altitudes (nearly a factor of four). The fact that a direct relationship between H_2O and OH was not observed at high and low altitudes is, we believe, due to more complicated chemistry occurring near ground elevations (e.g., higher background NO_2 and hydrocarbon concentrations). Unfortunately, background NO_2 concentrations could not be measured by MRI (the sensitivity of the NO_2 instrument used was 5 ppb NO_2: recently quoted background levels for NO_2 are in the ppt range).

---

*The Dasibi ozone analyzer, although sold to us as a proven aircraft instrument, was found to be unsuited to the Electra aircraft environment. More recent modifications have improved the performance of this instrument under flying conditions.

**On an absolute scale, we believe it quite unlikely that the OH data reported here could be in error by more than a factor of 2.5. Continued refinement of the calibration procedure as well as other aspects of the technique should further reduce the possible systematic error of the system in the future to levels of 20-25%.

Table I

SUMMARY OF OH AND RELATED DATA RECORDED ON JULY 16 ELECTRA FLIGHT

	Geographical Location	Time of Sampling	Total Integ. Time of Average Value	Altitude (above sea lev.)	Conc.	Signal/ Noise
OH	Over Rocky Mtns. between Denver & Farm., N.M.	1000-1020	10 min	6.0 km	3.3×10^6	∿ 4:1
	SW of Four Corners	1030-1045	8 min	2.1 km	9.2×10^6	∿ 4:1
	SW of Four Corners	1045-1100	8 min	2.1 km	8.1×10^6	∿ 4:1
	SW of Four Corners	1100-1115	8 min	2.1 km	11.0×10^6	∿ 5:1
O_3*	Non-plume bkgrd. levels near Four Corners	0959-1006	3 min	2.0 km	75 ppb	>10:1
	Non-plume bkgrd. levels near Four Corners	1024-1032	4 min	2.0 km	70 ppb	>10:1
	Non-plume bkgrd. levels near Four Corners	1226-1240	4 min	2.0 km	82 ppb	>10:1
H_2O	Over Rocky Mtns. between Denver & Farm., N.M.	1000-1020	10 min	6.0 km	2.0 Torr	>10:1
	SW of Four Corners	1030-1045	8 min	2.1 km	8.5 Torr	>10:1
	SW of Four Corners	1045-1100	8 min	2.1 km	8.5 Torr	>10:1
	SW of Four Corners	1100-1115	8 min	2.1 km	8.5 Torr	>10:1
CO	SW of Four Corners	1026	Grab Sample	2.1 km	---	>10:1
	SW of Four Corners	1058	Grab Sample	2.1 km	.24 ppm	>10:1
	Over Rocky Mtns. between Denver & Farm., N.M.	1300	Grab Sample	5.0 km	.23 ppm	>10:1

*Data reported by MRI. Integration times reported in table are non-plume sampling times.

Table I (Continued)

	Geographical Location	Time of Sampling	Total Integ. Time of Average Value	Altitude (above sea lev.)	Conc.	Signal/ Noise
CH_4	SW of Four Corners	1026	Grab Sample	2.1 km	--	>10:1
	SW of Four Corners	1058	Grab Sample	2.1 km	1.67 ppm	>10:1
	Over Rocky Mtns. between Denver & Farm., N.M.	1300	Grab Sample	5.0 km	1.68 ppm	>10:1
H_2	SW of Four Corners	1300	Grab Sample	2.1 km	.57 ppm	>10:1
	SW of Four Corners	1058	Grab Sample	2.1 km	.49 ppm	>10:1
	Over Rocky Mtns. between Denver & Farm., N.M.	1300	Grab Sample	5.0 km	.49 ppm	>10:1
N_2O	SW of Four Corners	1026	Grab Sample	2.1 km	.33 ppm	>10:1
	SW of Four Corners	1058	Grab Sample	2.1 km	.31 ppm	>10:1
	Over Rocky Mtns. between Denver & Farm., N.M.	1300	Grab Sample	5.0 km	.31 ppm	>10:1

UV FLUX*

Central Wavelength	Time of Day	Altitude (above sea lev.)	Flux Reading** ($10^{-5}W/cm^2$-nm)	J Value (O^1D Prod.) ($10^{-6}s^{-1}nm^{-1}$)
290.7 nm	1338	2.1 km	.02	.4
297.8 nm	1338	2.1 km	.20	1.4
305.3 nm	1338	2.1 km	.52	3.6
310.3 nm	1338	2.1 km	1.39	1.5
319.3 nm	1338	2.1 km	3.42	.05
329.2 nm	1338	2.1 km	6.81	.005
Integrated J value over entire bandwidth 285-320; $4.7\pm1.6\times10^{-5}s^{-1}$ +				

*Data recorded over New Mexico, north-western Texas and southern Colorado on August 1, 1976. For a detailed discussion of how these results were arrived at, see reference to Sellers et al (1977).

**Data corrected for albedo.

+The integrated J value one hour earlier at an altitude of 6 km was $5.6\times10^{-5}s^{-1}$, or 20% higher.

Section V

DISCUSSION OF RESULTS

Two basic questions can be examined concerning the July 16 OH data: (1) How do the OH values measured compare with those predicted by simple photochemical theories; and (2) What do these measured values of OH tell us about the conversion rate of SO_2 to sulfur aerosol and NO_2 to nitric acid. Both questions will be examined here in some detail.

COMPARISON OF MEASUREMENTS WITH THEORY

The OH free radical in the troposphere is believed to have its primary source in the photolysis of O_3 in the spectral region of 2850-3180Å.* The key steps are:

$$(1)\quad O_3 + h\nu \longrightarrow O(^1D) + O_2$$

$$(2)\quad O(^1D) + N_2 \longrightarrow O(^3P) + N_2^{\ddagger}$$

$$(3)\quad O(^1D) + H_2O \longrightarrow 2\ OH$$

On the basis of the above reaction scheme, three major points can be made:

(a) OH production in the atmosphere is strictly a daytime process.

(b) Summertime conditions are the most important for OH formation due both to the higher solar flux and H_2O levels available.

(c) Because of the competitive nature of reactions (2) and (3), the absolute concentration of atmospheric H_2O, not the relative humidity, is the critical parameter which influences the rate of production of OH.

Possible loss mechanisms for atmospheric OH include reactions (4)-(9), i.e.,

$$(4)\quad OH + CH_4 \longrightarrow CH_3 + H_2O$$

$$(5)\quad OH + CO \longrightarrow CO_2 + H$$

$$(6)\quad OH + NO_2 \xrightarrow{M} HNO_3$$

---

*In the case of a power plant plume, it is also possible that very low levels of OH could be produced via the photolysis of small amounts of HNO_2. The latter compound would be produced by heterogeneous processes involving NO, NO_2, and H_2C.

$$(7)\quad OH + SO_2 \xrightarrow{M} HSO_3$$

$$(8)\quad OH + RH \longrightarrow H_2O + R$$

$$(9)\quad OH + HO_2 \longrightarrow H_2O + O_2$$

For unperturbed tropospheric conditions,* reactions (4) and (5) dominate the loss path for OH; whereas, for strongly perturbed air resulting from anthropogenic emissions, processes (6) and (8) probably become dominate.

A further complication involved in defining the steady state atmospheric OH concentration is the existing uncertainty in the methane degradation cycle. Although the first step is obviously reaction (4), the nature of the subsequent degradation process for CH_3 going to CO is unclear. At the present time, this important chemistry must be summarized in the form of process (10),

$$(10)\quad CH_3 + O_2 \xrightarrow[\text{Steps}]{\text{Multi-}} X\ OH + CO + H_2O$$

The critical quantity in the above multi-step reaction is the coefficient "X". If X=0, then process (4) consumes OH radicals. If X=1, process (4) has little or no effect on the steady state concentration. Finally, if X>1, process (4) is a net OH source. At the present time, there is insufficient kinetic rate data to determine the value of the coefficient "X"; and it is quite likely that this quantity may best be identified via direct measurements of OH along with the related variables O_3, H_2O, UV, NO_2, NO, CO, CH_4, and higher hydrocarbons.

As an initial test of the agreement between observation and theory, the assumption will be made that in the countryside surrounding the Four Corners Power Plant, very low levels of NO, NO_2, and hydrocarbons are present. To a first approximation, we can then take processes (1), (2), (3), (4), and (5) as controlling the photochemical equilibrium level of OH. For the case where the coefficient "X" is set equal to zero, the appropriate equations, rate constants, and concentration terms are as follows:

$$[OH] = [O(^1D)] \times \left(\frac{2\ k_3[H_2O]}{k_5[CO] - (X-1)k_4[CH_4]} \right) \qquad (V)$$

$$[O(^1D)] = \frac{J_1[O_3]}{k_2[N_2] + k_3[H_2O]} \qquad (VI)$$

*It may well be that this unperturbed state of the atmosphere exists nowhere in the boundaries of the USA.

		Source of Information
Thus when:	$^{*}J_1 = 4.7\times10^{-5}s^{-1}$ (at 11:00 A.M.),	Table I
	$[O_3]_{Ave.} = 1.7\times10^{12}$ molec/cm^3,	Table I
	$k_2 = 5\times10^{-11}$ cm^{3}molec^{-1}s^{-1} (300 K),	NBS Circular 866
	$k_3 = 3.5\times10^{-10}$ cm^{3}molec^{-1}s^{-1} (300 K),	NBS Circular 866
	$[H_2O] = 2.0\times10^{17}$ molec/cm^3,	Table I
	and the altitude $\simeq$ 2 km	Table I
via eq. VI	$[O(^1D)] = 7.5\times10^{-2}$ molec/cm^3 .	

If then:		Source of Information
	X = 0,	
	$k_4 = 7.0\times10^{-15}$ cm^{3}molec^{-1}s^{-1} (300 K),	NBS Circular 866
	$k_5 = 1.5\times10^{-15}$ cm^{3}molec^{-1}s^{-1} (300 K),	NBS Circular 866
	$[CO] = 4.8\times10^{12}$ molec/cm^3,	Table I
	and $[CH_4] = 3.5\times10^{13}$ molec/cm^3	Table I
via eq. V	$[OH] = 1.1\times10^{7}$/cm^3 .	

For the case X = 1, i.e., each $CH_3 \rightarrow$ 1 OH

eq. V gives: $[OH] = 1.5\times10^{7}$/cm^3

For the case X = 2, i.e., each $CH_3 \rightarrow$ 2 OH

eq. V gives: $[OH] = 2.2\times10^{7}$/cm^3

In the previous calculations, the NO_2 background concentration was taken to be in the parts per trillion range. Under these conditions, the following chemistry is likely:

$$OH + CO \longrightarrow CO_2 + H$$

$$H + O_2 + M \longrightarrow HO_2 + M$$

$$HO_2 + HO_2 \xrightarrow{M} H_2O_2 + O_2$$

---

*J_1 at 11:00 A.M. should not be much different than J_1 at 1:30 P.M. as evaluated experimentally by Panametrics (Sellers, 1977).

Thus, CO is a major loss path for OH. If, however, the NO_2 background is taken to be several parts per billion, then it follows that:

$$OH + CO \longrightarrow CO_2 + H$$

$$H + O_2 + M \longrightarrow HO_2$$

$$\text{Equilib.} \quad NO_2 \rightleftharpoons NO \ (O_3, h\nu)$$

$$HO_2 + NO \longrightarrow NO_2 + OH$$

In this case, CO acts far less efficiently as a loss path for OH since most of the HO_2 is recycled to form new OH via reaction with NO. NO_2 itself can then become a major loss path for OH via reaction (6).

A calculation of the OH concentration for the case where the $[NO_2] \simeq 4$ ppb and $X = 0$ is given in the form of equation VIIa,

$$[OH] = [O(^1D)] \times \left(\frac{2k_3[H_2O]}{k_6[NO_2]M + k_4[CH_4]} \right) \qquad \text{(VIIa)}$$

Taking then $[M]k_6 = 8\times10^{-12} cm^3 molec^{-1} s^{-1}$ NBS Circular 866

and $[NO_2] = 8.1\times10^{10}$ molec/cm^3 See above assumption

gives $[OH] = 1.2\times10^7/cm^3$.

The above calculation probably represents an upper limit for the OH concentration since CO would continue to act as a minor loss path for OH. At 8 ppb NO_2, $[OH] = 6.9\times10^6/cm^3$.

For the case where $NO_2 = 4$ ppb and highly reactive hydrocarbons are present at the level of 4 ppb, the OH concentration can be calculated from equation VIIb.

$$[OH] = [O(^1D)] \times \left(\frac{2k_3[H_2O]}{k_6[NO_2]M + k_8[RH] + k_4[CH_4]} \right) \qquad \text{(VIIb)}$$

If $k_8 = 10^{-11}$ $cm^3 molec^{-1} s^{-1}$ (as is likely for highly reactive RH), then

$$[OH] = 6.25\times10^6/cm^3 .$$

The above calculation assumes that the R radical generated from reaction (8) would not result in the net production of OH.*

*It is difficult at this time to assess the reliability of this assumption and a sizeable uncertainty would necessarily have to be assigned to this calculation.

From the above calculations, it can be concluded that within the uncertainties of the photochemical model and the OH measurements good agreement exists. The OH measurements reported would favor the assignment of a value for the coefficient for X of 0 or 1; however, the lack of good background data on NO_2 and the absence of detailed information on reactive hydrocarbons precludes a more refined comparison between theory and measurements.

CALCULATION OF CONVERSION RATES FOR SO_2 AND NO_2 VIA REACTION WITH OH

SO_2 Lifetime Calculations

The basic reaction defining the atmospheric lifetime of SO_2 (in terms of homogeneous gas phase chemistry) is process (7),

$$OH + SO_2 + M \longrightarrow HSO_3 + M$$

The assumption made here is that the HSO_3 radical, which would be converted sequentially into HSO_5 and HSO_4 radicals, would not consume additional SO_2 molecules. (The latter point will need to be proven in controlled laboratory kinetic studies.) Taking the above assumption, together with the specification that all chemistry following reaction (7) and leading to the formation of H_2SO_4 aerosol would proceed rapidly as compared to the rate of reaction (7), a rather simple mathematical expression can be derived which permits the calculation of the SO_2 conversion lifetime, e.g.,

$$\frac{-d[SO_2]}{dt} = k[M][OH][SO_2] \qquad \text{(VIII)}$$

where M = N_2 and O_2. Taking $\frac{d[M]}{dt} = 0$, and $\frac{d[OH]}{dt} \simeq 0$ (for short time intervals), equation VIII can be rewritten as

$$\frac{-d[SO_2]}{dt} = K[SO_2], \qquad \text{(IX)}$$

where $K = k[M][OH]$.

Integration of equation IX then gives

$$\frac{\ell n[SO_2]_0}{[SO_2]_t} = Kt \ ,$$

where $[SO_2]_0$ is the initial SO_2 concentration and $[SO_2]_t$ is the SO_2 concentration at some later time "t". The conversion lifetime is then defined by the condition

$$\frac{[SO_2]_0}{[SO_2]_t} = e = 2.7 \quad .$$

Thus, K is equal to 1/t or $\tau_{(\text{lifetime})} = \frac{1}{k[M][OH]}$. (X)

In calculating the conversion lifetime from equation X, two approaches can be taken: (a) the calculation can be based on a snap shot OH concentration or (b) the lifetime can be computed on the basis of a long time average OH concentration.

For method (a),

$$\tau_{SO_2} = \frac{1}{k_7[M][OH]} = 1.25\times10^5 \text{ s or } 1.4 \text{ days}$$

where $[M]k_7 = 9\times10^{-13}$ cm^3 molec^{-1}s^{-1}

and $[OH] = 9.4\times10^6/\text{cm}^3$.

Source of Information

Results from D.D.Davis et al. (Davis and Klauber, 1975)

Table I

Thus in this case the OH level is assumed to remain constant at $9.5\times10^6/\text{cm}^3$ throughout the time period of 1.4 days. In point of fact, the OH level varies significantly during a 24 hour day as is indicated in Figure 11. Hence, a more realistic calculation of the SO_2 lifetime (method b) can be carried out if an appropriate diurnal averaging factor is used in conjunction with the measured high noon OH concentration. From Figure 11, it can be seen that Chang et al have computed this diurnal factor, α, for an altitude of 1 km and summertime conditions at 30^{o}N latitude. The value reported, .32, is used here to readjust the measured value of OH which was made at $\sim$35^{o}N latitude. In this case $[OH]_{Ave.} = 2.94\times10^6$,

$$\tau_{SO_2} = \frac{1}{(9\times10^{13})(2.9\times10^6)} = 3.8\times10^5 \text{ s}$$

or

$$\tau_{SO_2} = 4.4 \text{ days.}$$

From this computation, it is apparent that even using a diurnally averaged [OH] the predicted lifetime for conversion of SO_2 to aerosol via reaction (7) is sufficiently short as to define a very important process. It may, in fact, be the dominate mechanism under daylight summertime conditions. A possible further decrease in the calculated conversion time for SO_2 may also result from new kinetic studies on reaction (7). For example, there is now some evidence which

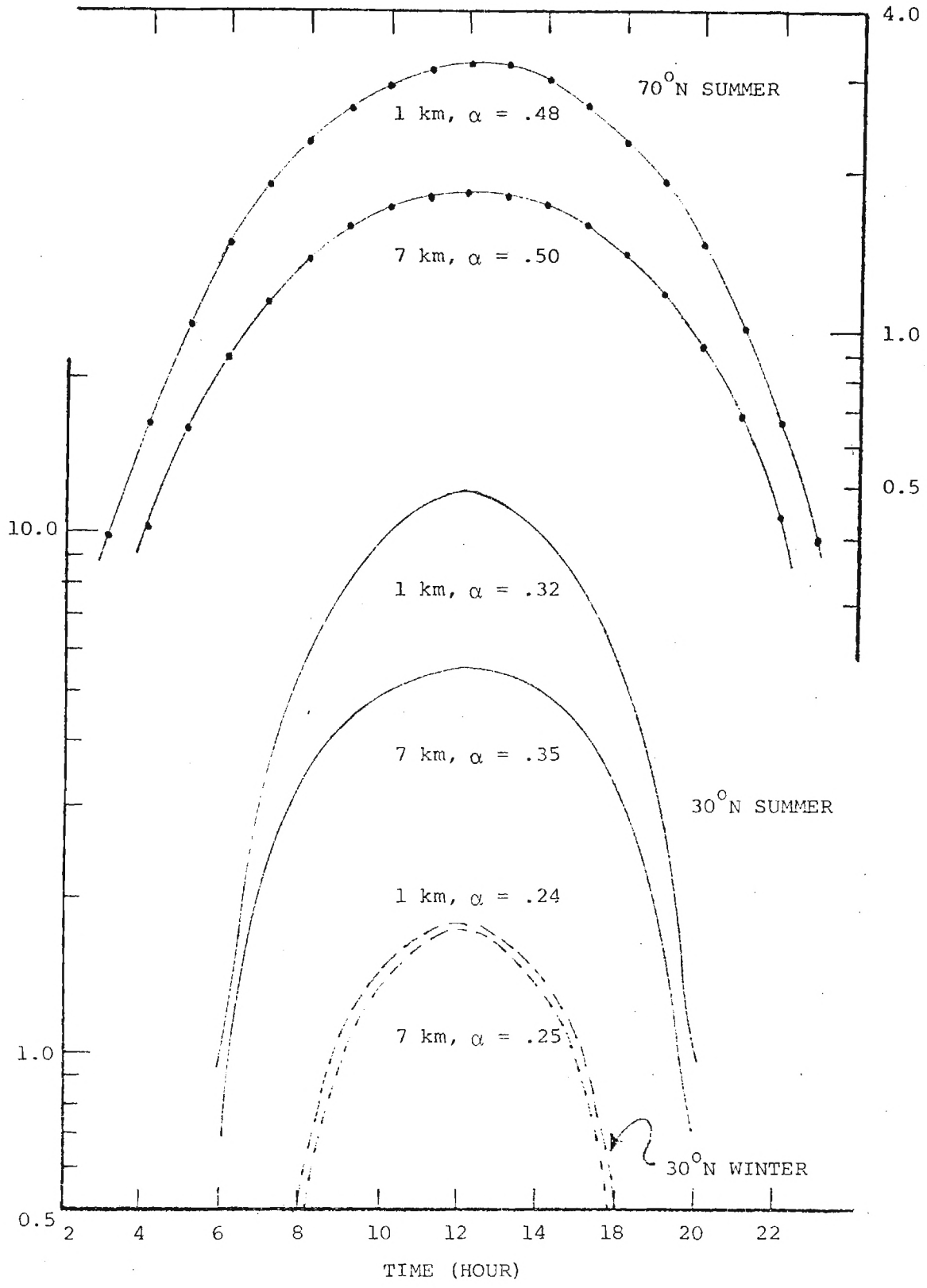

Figure 11. (Chang, Wuebbles, and Davis, 1977) Diurnal fluctuations in the steady state concentration of atmospheric OH as a function of latitude and altitude. (α = diurnal averaging factor)

suggests that k_7 could be as much as 1.5 times higher than the value used in these calculations.

NO_2 Lifetime Calculations

The reaction of importance here is

$$OH + NO + M \longrightarrow HNO_3 + M \quad .$$

The appropriate rate expression for the conversion of NO_2 to HNO_3 is, therefore,

$$\frac{-d[NO_2]}{dt} = k_6[NO_2][OH] \quad .$$

Using the same assumptions employed for the SO_2 lifetime calculation, we have

$$\tau_{NO_2} = \frac{1}{k_6[M][OH]} = 1.34\times10^{4} \text{ s or } 3.61 \text{ hours} \quad .$$

where $k_6[M] = 8\times10^{-12}$ $\qquad M = N_2 + O_2$.

In the above case, the calculated lifetime for NO_2 is short, the snap shot concentration measurement of OH is more realistic than the diurnally averaged value. However, what is now needed are numerous OH concentration measurements as a function of both the time of day and the season.

Section VI

CONCLUSIONS

A. It has been demonstrated that an aircraft borne laser probe can successfully measure ambient levels of OH at near ground level altitudes for daylight summertime conditions involving moderate levels of humidity.

B. Although only limited OH data were collected during this program, the value of this data is still quite significant. These data strongly support the hypothesis that homogeneous chemistry, involving OH radicals in particular, is of major importance in defining both the NO_x and sulfur chemistry of power plant plumes. However, due to the strong dependence of the OH species on solar flux and the H_2O concentration, the relative importance of OH induced chemistry in a particular power plant plume will depend very significantly on the season of the year and the geographical location of the plant.

C. The fact that only near plume measurements of ambient OH were successfully made rather than in situ values does not alter the major conclusions arrived at in statement B, concerning SO_2 chemistry. Since the predicted conversion lifetime for SO_2 is three to four days, this necessarily means that over 90% of the conversion process would take place under extremely dilute plume conditions where the OH concentration would be that of ambient air and aerosol levels would probably be only slightly above ambient levels.

D. Because of the much larger rate constant for the reaction of OH with NO_2 versus SO_2 ($\sim$ a factor of 10), the conversion of NO_2 to HNO_3 will occur much more rapidly in a plume ($\sim$3 to 5 hours) than the corresponding conversion of SO_2 to H_2SO_4. As discussed earlier in the introduction, all OH induced chemistry has a pronounced induction period in a power plant plume due to the depletion of O_3 by NO (see Figure 1). The above calculations indicate that high levels of NO_x in the plume could also result in an additional induction period for the conversion of SO_2 to H_2SO_4.

Section VII

RECOMMENDATIONS

A. The OH data available at this point is very limited and must be substantially expanded upon. OH data must be collected not only as a function of the time of day and season of the year, but it must be generated at many different geographical locations in the USA.

B. To properly understand the significance of any future OH measurements, as related to power plant plumes, it will be most important that data are collected on such key variables as the UV flux (2850 to 3180A in 30Å bandwidths), H_2O, O_3, CO, CH_4, NO-NO_2 (background levels), and identified high molecular weight hydrocarbon concentrations.

C. In future flight programs in which the conversion time for SO_2 to aerosol is being examined via direct measurements of the OH radical concentration, it would be most significant if concurrent measurements could be made of the SO_2 and sulfate aerosol levels. The latter measurements could provide an independent measurement of the chemical conversion of SO_2 to aerosol. Unfortunately, in the reported Four Corners Study, the SO_2-sulfate data base generated by MRI was totally inadequate for purposes of computing SO_2 conversion rates.

D. If in-plume OH concentrations are to be measured in future flight programs (i.e., to better establish the NO_2 to HNO_3 conversion time), it will be necessary to increase the on and off OH resonance cycling time by at least a factor of 100-1000 over that used in our 1976 study (e.g., 5 sec). With this time resolution, aerosol variations would not appear as an oscillating noise signal. We believe that this technological feat could be accomplished with (1) a $12,000 modification to our existing driver laser; and (2) the addition of a second dye laser module ($20K) to the already existing system. The modification to our driver laser would permit the unit to operate in a double pulsing mode with the pulse separation being ~100 microseconds. These two independent laser pulses could then be separated and directed into two identical dye lasers. One of these dye lasers would be

tuned, after frequency doubling, to the OH resonance frequency; the second would be shifted off resonance by $\sim .08\text{Å}$ to measure the noise signal only. Thus, measurements of the on and off OH resonance frequency signals would occur in a time period of only 100 microseconds.

REFERENCES

Chang, J., D. Wuebbles, and D.D. Davis, 1977. "A Theoretical Model of Global Tropospheric OH Distributions," 3, Geophysical Res. (in press).

Davis, D.D., G. Smith, and G. Klauber, 1974. "Trace Gas Analysis of Power Plant Plumes via Aircraft Measurements: O_3, NO_x, and SO_2 Chemistry," Science 186: 773.

Davis, D.D., and G. Klauber, 1975. "Atmospheric Gas-Phase Oxidation Mechanisms for the Molecule SO_2," proceedings of the Symposium on Chemical Kinetics Data for the Upper and Lower Atmosphere, International Journal of Chemical Kinetics Symposium #1.

Davis, D.D., 1977. "Atmospheric Fate of SO_2 in Power Plant Plumes," Aerial Techniques for Environmental Monitoring Symposium, Las Vegas, Nevada, March, 1977.

Davis, D.D., W. Heaps, and T. McGee, 1976. "Direct Measurements of the Natural Tropospheric Levels of OH via an Aircraft Borne Tunable Dye Laser," Geophys. Res. Letters, Vol. 3, p. 331.

Davis, D.D., W. Heaps, T. McGee, A. Nelson, and P. Wine, 1977. "An Air-borne Laser Induced Fluorescence Apparatus for Measuring Trace Gases at the parts per quaddrillion to parts per trillion Range," submitted to J. Applied Optics.

Husar, R., 1977. "Power Plant Plume Characteristics," proceedings of the Aerial Techniques for Environmental Monitoring Symposium, Las Vegas, Nevada, March, 1977.

Kiang, C.S., D. Stauffer, V.A. Mohnen, J. Bricard, and D. Vigla, 1973. "Hetero-molecular Nucleation Theory Applied to Gas-to-Particle Conversion," Atmos. Environ., 1, p. 1279.

Kiang, C.S., V.A. Mohnen, D. Stauffer, P. Hamill, and G.H. Walker, 1974. "Removal Processes of Atmospheric Aerosols and Gases Involving Nucleation Mechanisms," Proc. Precipitation Scavenging, p. 233-46.

Moriarty, A., W. Heaps, and D.D. Davis, 1976. "A Frequency Doubled Pressure-Tunable Oscillator-Amplifier Dye Laser System," Optics Communications, Vol. 16, p. 324.

NBS Circular 866, 1975. "Chemical Kinetic and Photochemical Data for Modelling Atmospheric Chemistry," edited by R.F. Hampson, Jr. and D. Garvin.

Newman, L., and J. Forrest, 1977. "Further Studies on the Oxidation of Sulfur Dioxide in Coal-Fired Power Plant Plumes," Atmos. Environ. (in press).

Sellers, B. and F. Hansen, 1977. "Measurements of Tropospheric 300 nm Solar UV Flux: Determination of the Rate of Production of $O(^1D)$," J. Atm. Science (in press).